Tropospheric Ozone Production Pathways with Detailed Chemical Mechanisms

Dissertation zur Erlangung des akademischen Grades
des Doktors der Naturwissenschaftern
am Fachbereich Geowissenschaften
an der Freien Universität Berlin

Vorgelegt von
Jane Coates
im Juli 2016

Freie Universität Berlin

1. Gutachter: Dr. Tim Butler
2. Gutachter: Prof. Dr. Peter Builtjes
3. Gutachter: Prof. Dr. Ulrike Langematz

Abstract

Acknowledgements

Table of Contents

List of Tables

List of Figures

Chapter 1

Introduction

Ozone (O_3) is an atmospheric constituent gas found in the stratosphere and troposphere, however its atmospheric effects are very different in these distinct regions. About 90% of the atmospheric ozone is present in the stratosphere, with a peak mixing ratio of about 12 ppm (Seinfeld and Pandis, 2006). Stratospheric ozone absorbs the sun's ultraviolet radiation in the wavelength region 280 - 315 nm, this is extremely important as excess UV radiation can cause skin cancer, cataracts and a suppressed immune system in humans and can also damage plant, single-cell organisms and aquatic ecosystems (World Meteorological Organisation, 2011).

In contrast, tropospheric ozone that is found close to the surface is both a pollutant and a greenhouse gas. Increased levels of tropospheric ozone are harmful to humans, plants and other living systems, as high ozone exposure can lead to pulmonary problems in humans and can decrease both crop yields and forest growth (World Meteorological Organisation, 2011).

Globally, tropospheric ozone is formed mainly via chemical production and downward transport from the stratosphere into the troposphere, called the Stratosphere-Troposphere Exchange (STE) may also play a role. The STE is driven by the Brewer-Dobson circulation (Brewer, 1949; Dobson, 1956). This is a relatively slow circulation (over a timescale of weeks to months) and is due to planetary wave disturbances in the troposphere (Haynes et al., 1991). The circulation causes air to move downward from the stratosphere into the troposphere at the mid at high latitudes and is balanced by upward exchange at the tropics. The STE also has a seasonal variability where the maximum transport occurs during spring (Appenzeller et al., 1996), due to the increase in altitude of the tropopause - the boundary level between the troposphere and the stratosphere - which moves stratospheric air into the troposphere.

A spring-time peak in O_3 concentration is common in many areas, especially in the midlatitude Northern Hemisphere, and it was originally thought that the STE was mainly responsible. However, it is only very rarely that O_3 originating via STE

can influence tropospheric O_3 levels (Lelieveld and Dentener, 2000). It was later realised that this spring maximum is due to the photochemical reactions occuring in the Northern Hemisphere spring after the buildup of reservoir species over winter (Penkett and Brice, 1986) that are then oxidised photochemically, the increase in these reactions is due to the increase in temperature, moisture and sunlight. Hence, photochemical reactions are the major source of surface tropospheric ozone (Lelieveld and Dentener, 2000) and since O_3 is produced in this way it is termed a secondary pollutant.

Tropospheric O_3 is not only impacted by emission levels, it is also affected by meteorological variables such as temperature, number of hours of sunshine and wind as these impact transport, dry and wet deposition rates and also chemical reaction rates (Hess and Mahowald, 2009). Meteorology influences both regional and global O_3 (Hess and Mahowald, 2009), climate patterns such as El Niño are also known to impact O_3 levels in certain areas (Sudo and Takashi, 2001).

The effect of meteorology is an aspect of atmospheric chemical transport modelling that needs to be taken into account. However it is also frequently the major source of uncertainty for the calculated O_3 concentrations. Wind speeds in particular may lead to under- or over-predicated values of O_3 concentrations (Sillman, 1999).

In general, there is great effort to reduce anthropogenic emissions that impact air quality and human health. For example, the EPA in the US and European Union all have regulations related to air quality with a set exceedance limit for O_3 concentrations. Many cities in the US, especially in the northeast and southern California, have reduced the emissions of O_3 precursors - mainly volatile organic compounds (VOC) emissions - due to repeated exceedances (Fiore et al., 1998). These VOC emission reductions have proven successful as the amount of O_3 in these metropolitan areas has been decreased despite nitrogen oxide levels, which also impact O_3 levels, being almost constant (Fiore et al., 1998; Lin et al., 2001).

Modelling of O_3 has greatly influenced the understanding of complexity of atmospheric chemistry, for example the non-linear relationship of O_3 production on the VOC and nitrogen oxides concentrations. This in turn has led to a better understanding on how to reduce the O_3 levels for better air quality. The need for more realistic and effective air quality standards in turn also drives the model development and deeper understanding of atmospheric chemistry. Providing detailed information of which VOCs can produce the most O_3 is of greater benefit for regulation purposes rather than lumping all VOCs under one common regulation. Moreover, this can give indication on possibly replacement substances in order to improve air quality.

1.1 Tropospheric Chemistry

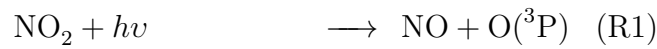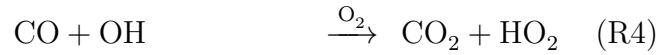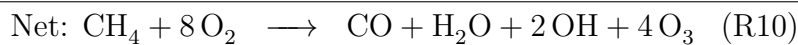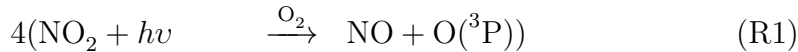### 1.1.1 Ozone Chemistry

Troposperic ozone is principally formed by the photolysis of nitrogen dioxide (NO_2), which produces nitrogen oxide (NO) and a ground state oxygen atom ($O(^3P)$), this then reacts with molecular oxygen (O_2) to form O_3. Ozone reacts rapidly with NO to return NO_2 and O_2, this is represented by the following reaction cycle.

$$
\begin{aligned}
NO_2 + h\upsilon &\longrightarrow NO + O(^3P) \quad &(R1) \\
O(^3P) + O_2 &\xrightarrow{M} O_3 \quad &(R2) \\
NO + O_3 &\longrightarrow NO_2 + O_2 \quad &(R3)
\end{aligned}
$$
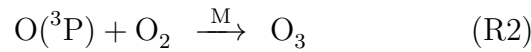
These reactions do not produce net O_3, due to a photoequilibrium between NO, NO_2 and O_3 (Atkinson, 2000). Adding VOCs of both biogenic and anthropogenic origin, such as methane (CH_4), and other gas-phase compounds, such as carbon monoxide (CO) - to the mix, results in net O_3 production. The oxidation mechanism of CO, taking into account reactions that give maximum O_3 yield, is

$$
\begin{aligned}
CO + OH &\xrightarrow{O_2} CO_2 + HO_2 \quad &(R4) \\
HO_2 + NO &\longrightarrow NO_2 + OH \quad &(R5) \\
NO_2 + h\upsilon &\longrightarrow NO + O(^3P) \quad &(R1) \\
\hline
\text{Net: } CO + 2\,O_2 + h\upsilon &\longrightarrow CO_2 + O_3 \quad &(R6)
\end{aligned}
$$

whilst the oxidation mechanism of CH_4 with maximum O_3 yield is

$$
\begin{aligned}
CH_4 + OH &\xrightarrow{O_2} CH_3O_2 + H_2O \quad &(R7) \\
CH_3O_2 + NO &\xrightarrow{O_2} HCHO + HO_2 + NO_2 \quad &(R8) \\
HCHO + h\upsilon &\xrightarrow{2\,O_2} 2\,HO_2 + CO \quad &(R9) \\
3(HO_2 + NO &\longrightarrow NO_2 + OH) \quad &(R5) \\
4(NO_2 + h\upsilon &\xrightarrow{O_2} NO + O(^3P)) \quad &(R1) \\
\hline
\text{Net: } CH_4 + 8\,O_2 &\longrightarrow CO + H_2O + 2\,OH + 4\,O_3 \quad &(R10)
\end{aligned}
$$
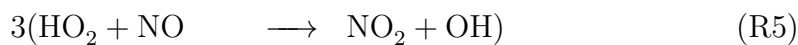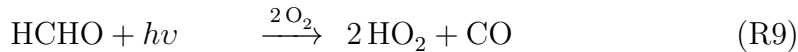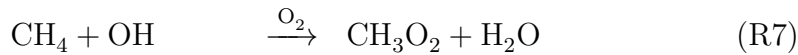
taking into account the net result for the CO oxidation mechanism (R6), the net yield for CH_4 is

$$
CH_4 + 10\,O_2 \longrightarrow CO_2 + H_2O + 2\,OH + 5\,O_3. \quad (R11)
$$
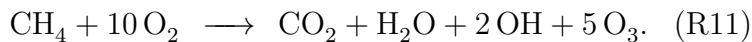
Both mechanisms are taken from (Seinfeld and Pandis, 2006).

To summarise, oxidation of VOCs results in the formation of peroxy radicals which then convert NO to NO_2 and both (R1) and (R2) proceed. These oxidation mechanisms are linked in the sense that the CH_4 mechanism gives a maximum O_3 yield, once the mechanism of CO is also included.

Symbol	Family Name	Components
NO_x	Nitrogen oxides	$NO + NO_2$
O_x	Odd oxygen	$O_3 + O + O(^1D) + NO_2 + NO_3 + N_2O_5$
NO_y	Oxidised nitrogen	$NO + NO_2 + HNO_3 + N_2O_5 + ClONO_2$ $+ NO_3 + HOONO_2 + BrONO_2$
HO_x	Hydrogen radicals	$OH + HO_2$
PAN	Peroxyacyl nitrates	Compounds of general formula $RC(O)OONO_2$

Table 1.1: Chemical Families commonly used in Tropospheric Chemistry (Seinfeld and Pandis, 2006)

Since these mechanisms produce the maximum O_3 yield, the reactions that cause O_3 destruction or inhibit its production are not included. It should also be noted that some reactions can follow more than one pathway that is indicated above and that products from these pathways can be removed from the atmosphere via deposition processes. Thus, the maximum O_3 yield outlined in reactions (R6) and (R11) is not reached in the atmosphere.

Another aspect of O_3 production is its dependence on the atmospheric concentrations of both VOCs and nitrogen oxides ($NO_x = NO + NO_2$) and this also influences the reaction pathways. Moreover, the precursors of ozone are linked to anthropogenic activity, hence a so-called weekend effect (i.e. there is a reduction on O_3 concentration over the weekend) is also evident (see for example, (Koo et al., 2012)). Further discussion on the balance of VOC and NO_x concentration to O_3 production shall be given in Section 1.1.6.

1.1.2   Chemical Families

A concept that is extremely useful in atmospheric chemistry is that of a chemical family. This is used to describe two or more compounds that form a rapid cycle of production and destruction. An example is the cycling between NO and NO_2 in (R1) and (R3), hence NO and NO_2 form the nitrogen oxides chemical family NO_x.

A chemical family also has its own chemical lifetime, where the chemical lifetime is the average time that a chemical species takes to be removed - by reaction or deposition processes - from the atmosphere. An equilibrium is reached for the compounds of the chemical family, called a pseudo-steady state, which is then re-balanced when a compound from the family reacts with a species not present in the chemical family.

Examples of important chemical families are given below in Table 1.1 and taken from (Seinfeld and Pandis, 2006).

1.1.3 Reservoir Molecules

Compounds that react with radicals or NO_x are called reservoir molecules. These will slow down O_3 production and if they have a sufficiently long enough lifetime, can also transport and then release radicals or NO_x to promote O_3 formation in a separate location. For example, hydrogen peroxide (H_2O_2) is a reservoir molecule for HO_x as shown in the below sequence of reactions (Seinfeld and Pandis, 2006).

$$HO_2 + HO_2 \longrightarrow H_2O_2 + O_2 \quad \text{(R12)}$$
$$H_2O_2 + h\upsilon \longrightarrow OH + OH \quad \text{(R13)}$$
$$H_2O_2 + OH \longrightarrow H_2O + HO_2 \quad \text{(R14)}$$

Nitrous acid (HONO) is a reservoir molecule for NO_x and HO_x, formed by a heterogeneous reaction of NO_2 and H_2O. HONO can be formed during night-time and then photodissociates at sunrise to regenerate OH and NO (Seinfeld and Pandis, 2006).

$$HONO + h\upsilon \longrightarrow OH + NO \quad \text{(R15)}$$
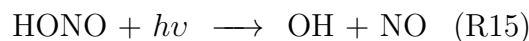
An important class of reservoir molecules are ther peroxyacyl nitrates (PANs) of general formula $RC(O)OONO_2$. The first compound in this class, $CH_3C(O)OONO_2$, is also called PAN and can be formed by reactions of peroxyacetyl radicals with NO_2, PAN then thermally dissociates to return the reactants (Kleinman, 2005).

$$CH_3C(O)O_2 + NO_2 + M \rightleftharpoons CH_3C(O)OONO_2 + M \quad \text{(R16)}$$
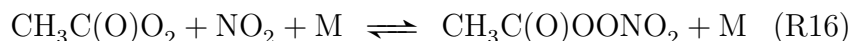
PAN's lifetime is dependent on meteorology due to a strong temperature dependence (Moxim et al., 1996). This can lead to situations where NO_x is transported to different regions and then released by dissociation. PAN is thought to have a regional rather than a global influence on the NO_x budget (Moxim et al., 1996).

1.1.4 Volatile Organic Compounds

Table 1.2 lists Non-Methane Volatile Organic Compounds (NMVOCs) that are emitted from US cities (Baker et al., 2008). The mean is calculated from (Baker et al., 2008) using the total of 31 data points from 28 cities in the United States. Of these NMVOCs there is only one which has a primarily biogenic source and this is isoprene (2-methyl 1,3-butadiene). Although not evident from Table 1.2, biogenic VOCs are globally the most abundant VOCs (Goldstein and Galbally, 2007). Since the data in Table 1.2 are mainly taken from urban cities, the impact of anthropogenic emissions outweigh those of the biogenic sources (Baker et al., 2008) - although isoprene has some anthropogenic sources (see (Borbon et al., 2003)).

The sources of the alkanes listed below are natural gases, liquified petroleum gas (LPG), combustion and industry, for the case of octane, vehicle exhaust is also a

Table 1.2: NMVOCs emitted from US cities (Baker et al., 2008)

source. Alkene sources are mainly due to industrial activities and vehicular emissions. Aromatic compounds are mainly due to vehicle emissions, while benzene and toluene are also emitted due to industrial activity and combustion is also a further source for benzene (Arsene et al., 2009).

Alkanes are saturated hydrocarbons, meaning that all bonds between carbon and hydrogen atoms are single bonds, resulting in slow reacting species. The dominant tropospheric process for alkanes is reaction with the hydroxyl (OH) radical, but they also react with the nitrate (NO_3) radical and chlorine atoms. The presence of a double bond in alkenes and a triple bond in alkynes leads to increased reactivity. In the troposphere both alkenes and alkynes react with the OH radical, the NO_3 radical and also with O_3. Aromatic compounds react with the OH and NO_3 radicals. Hence it can be noted that the key reactive species in the troposphere is the OH radical as it reacts with practically all organic compounds, the exceptions being chlorofluorocarbons (CFCs) and halons without hydrogen atoms.

Reaction with the OH radical is predominant during the day, since it is formed mainly by photolysis, during the night there is an increase in the NO_3 radical concentration and so reaction rates with this radical are increased. The reason for this increased night-time concentration of the NO_3 radical is that during the day the reaction that forms NO_3

$$NO_2 + O_3 \longrightarrow NO_3 + O_2 \quad (R17)$$

is balanced by the quick photolysis of NO_3

$$NO_3 + h\upsilon \longrightarrow NO + O_2 \qquad (R18)$$
$$NO_3 + h\upsilon \longrightarrow NO_2 + O(^3P). \quad (R19)$$

The main photolysis pathway is via reaction (R19) which occurs about 90% of the time. However, during night-time photolysis does not occur and hence there is a buildup of NO_3 radicals (Atkinson, 1990, 2000).

1.1.5   VOC Chemistry

Figure 1.1 represents a general and simplified reaction scheme for VOCs in the troposphere. Although there are many different VOC classes involved in tropospheric chemistry, there are many similarities between their reaction schemes. This shall be summarised below however for more a more detailed description of tropospheric chemistry, (Atkinson, 2000) should be consulted.

As noted earlier, the most common initiation reaction of a VOC is with the OH radical, and this forms an alkyl or substituted alkyl radical (R) depending on
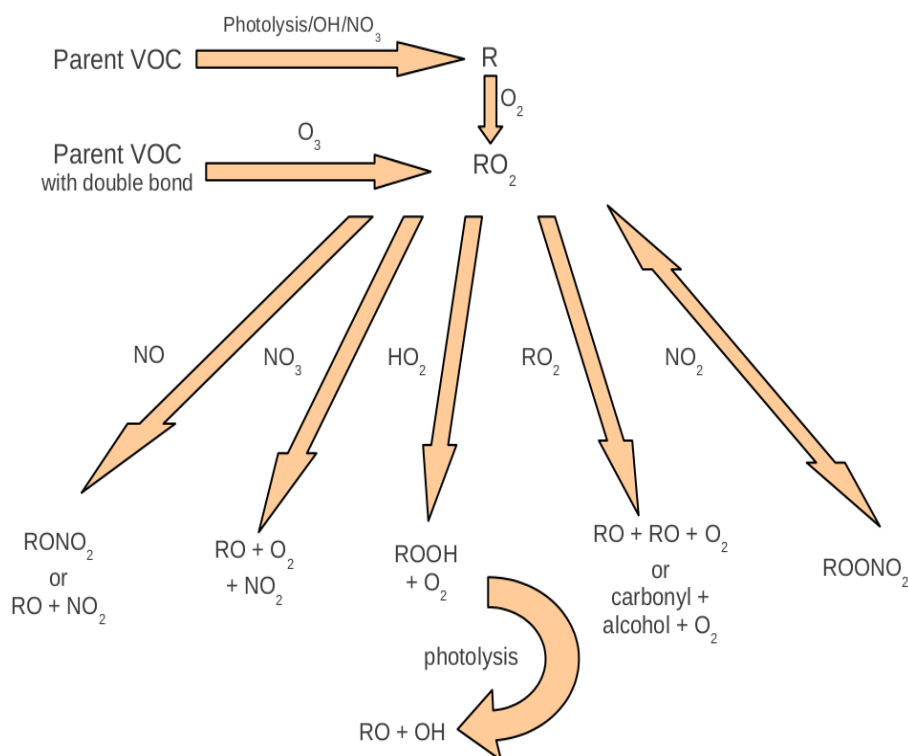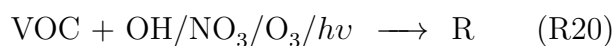
Figure 1.1: VOC reaction pathway

the parent VOC. The addition reaction with O_2 then leads to the formation of alkyl peroxy radicals (RO_2). During the night-time, reaction with the NO_3 radical is of importance and for VOCs containing a double bond, reaction with O_3 also occurs. Photolysis is an important degradation initiator for carbonyl species, this is particularly important throughout the whole degradation mechanism of the VOC as carbonyl species, such as formaldehyde, are common reaction products. These initial reaction pathways all lead to the formation of RO_2 radicals, as shown below.

$$\text{VOC} + \text{OH}/\text{NO}_3/\text{O}_3/h\upsilon \longrightarrow \text{R} \qquad \text{(R20)}$$
$$\text{R} + \text{O}_2 \longrightarrow \text{RO}_2 \quad \text{(R21)}$$

RO_2 radicals can subsequently react with NO, NO_2, hydroperoxy (HO_2) radicals, NO_3 radicals - mainly during night-time - and also with other alkyl peroxy radicals. The competition between these reactions determines the amount of net ozone production or loss from the parent VOC.

$$
\begin{array}{llr}
\text{RO}_2 + \text{NO} + \text{M} & \longrightarrow \text{RONO}_2 + \text{M} & \text{(R22)} \\
\text{RO}_2 + \text{NO} & \longrightarrow \text{RO} + \text{NO}_2 & \text{(R23)} \\
\text{RO}_2 + \text{NO}_2 + \text{M} & \rightleftharpoons \text{ROONO}_2 + \text{M} & \text{(R24)} \\
\text{RO}_2 + \text{HO}_2 & \longrightarrow \text{ROOH} + \text{O}_2 & \text{(R25)} \\
\text{RO}_2 + \text{NO}_3 & \longrightarrow \text{RO} + \text{NO}_2 + \text{O}_2 & \text{(R26)} \\
\text{RCH(OO)R}' + \text{RCH(OO)R}' & \longrightarrow \text{RCH(O)R}' + \text{RCH(O)R}' + \text{O}_2 & \text{(R27)} \\
\text{RCH(OO)R}' + \text{RCH(OO)R}' & \longrightarrow \text{RCH(OH)R}' + \text{RC(O)R}' + \text{O}_2 & \text{(R28)}
\end{array}
$$

All pathways in Figure 1.1 that lead to NO_2 formation can result in O_3 formation due to (R1) and (R2). Reaction with the HO_2 radical results in the formation of hydroperoxides (ROOH), which then photolyse to an alkoxy (RO) radical and the OH radical, this OH radical is then available to react with other VOCs. The carbonyl and alcohol products resulting from reaction with other RO_2 radicals will follow a similar sequence of reactions and hence can also produce further O_3. Reaction with NO_2 leads to the formation of alkyl peroxynitrates ($ROONO_2$), however this reaction product can be thermally unstable and may decompose quickly to the reactants, as mentioned in Section 1.1.3.

The RO radical that results from many of the RO_2 pathways undergoes further reactions, either by decomposition, isomerisation or reaction with O_2. The products that result from the reaction pathways depend on the parent VOC and this also determines the number of NO-to-NO_2 conversions, eventually leading to O_3 formation.

All VOCs and their degradation products will ultimately result in carbon dioxide (CO_2) and water vapour. The path that each VOC takes to reach its final products is dependent on the type of VOC, the radical concentration, the NO_x concentration and other factors such as time of day and year. The detailed atmospheric chemistry of some simple VOCs is well-understood (for example, methane) however for more complex molecules, especially aromatic VOCs, there are a great number of uncertainties. These uncertainties can be related to kinetic data, photolysis rates, reaction branching ratios and in most cases the reaction products. Any uncertainties in reaction pathways and products of VOCs also leads to uncertainties in the ozone forming potential of the respective VOC (Atkinson, 2000).

1.1.6   VOC and NO_x Chemistry

As mentioned above, O_3 chemistry is influenced by both VOC and NO_x concentrations. Figure 1.2 depicts the non-linear relationship between O_3 concentration when considered as a function of VOC concentration (in ppmC, i.e. parts per million mass of a carbon unit of the VOC, $CH_{2.5}$) and NO_x concentration (in ppm, i.e. parts per million mass).

This relationship can be divided into distinct regimes: **NO_x-sensitive**, **VOC-sensitive** and **VOC-and-NO_x-sensitive**. The NO_x-sensitive regime is the right-most part, the VOC-and-NO_x-sensitive regime is the middle section and the VOC-sensitive regime is the left-most part of Figure 1.2 and these correspond to high, middle and low VOC:NO_x ratios, respectively. These different regimes arise from how the atmosphere removes NO_x and radicals resulting from VOCs.

In the NO_x-sensitive regime, the concentration of NO_x is low compared to that of radicals. Hence, peroxy radicals are removed by reaction with the OH radical such as
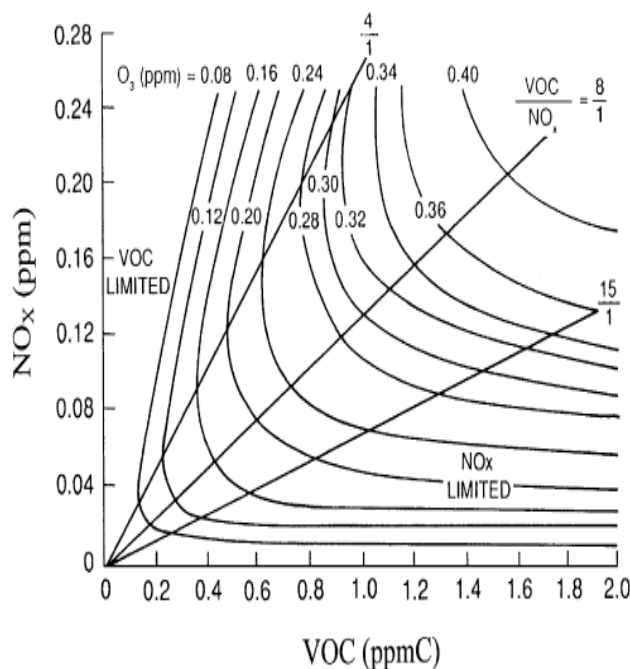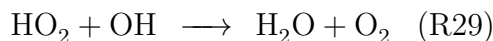
Figure 1.2: Ozone isopleth plots for various initial concentrations of NO_x and a specified VOC mixture. Taken from (Jenkin and Clemitshaw, 2000).

$$HO_2 + OH \longrightarrow H_2O + O_2 \quad (R29)$$

or by peroxy radical addition reactions.

$$HO_2 + HO_2 \longrightarrow H_2O_2 \qquad (R12)$$
$$RO_2 + HO_2 \longrightarrow ROOH + O_2 \quad (R25)$$

This results in the NO concentration controlling the number of NO-to-NO_2 conversions, rather than the concentration of peroxy radicals produced during VOC oxidation. An increase in NO conversion would thus promote O_3 production due to an increase in (R1) and (R2) reactions. Increasing VOC concentrations would not increase O_3 production as this only speeds up the formation of peroxy radicals and has no direct effect on the NO_x concentration.

The VOC-sensitive regime corresponds to high NO_x concentrations, hence radicals will tend to react with either NO or NO_2. Increasing NO_x concentrations will not increase not increase O_3 production as the NO_x will react with the peroxy radicals resulting from VOC degradation. However, this increase in NO_x increases the formation of nitric acid (HNO_3) by reaction with the OH radical (Kleinman, 1991, 1994; Kirchner et al., 2001).

$$OH + NO_2 \longrightarrow HNO_3 \quad (R30)$$
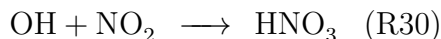
The competition of VOCs and NO_x for reaction with the OH radical is at the heart of O_3 production or destruction in the VOC-sensitive regime. Reaction of VOCs with
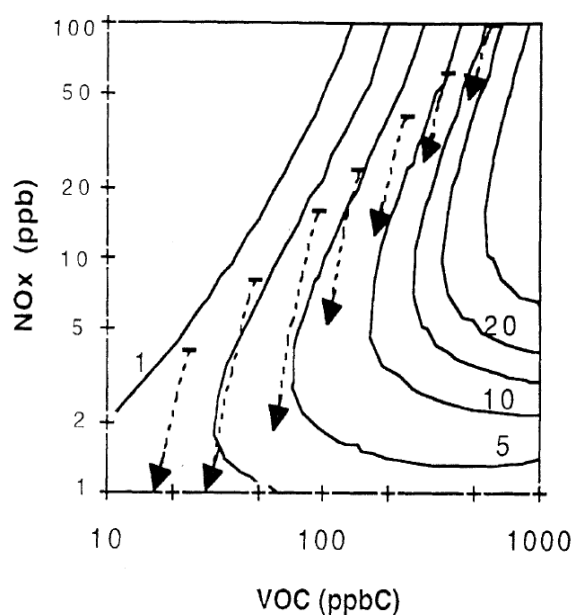
Figure 1.3: Air parcel evolution overlayed with ozone isopleth plots for various initial concentrations of NO_x and VOCs. Taken from (Sillman, 1999).

the OH radical will produce more peroxy radicals, increasing O_3 production whilst reaction of NO_x increases HNO_3 by (R30) which reduces O_3 production (Kleinman, 1991, 1994; Kirchner et al., 2001).

The VOC-and-NO_x-sensitive regime is characterised by O_3 production being sensitive to both VOC and NO_x concentrations. The turning point from a VOC-sensitive to a VOC-and-NO_x-sensitive regime is when the maximum O_3 production for a particular VOC concentration has been reached. The shift into a NO_x-sensitive occurs when increases in VOC concentrations result in very little O_3 production (Kirchner et al., 2001). The non-linear relationship can be thought of as a titration process between the amount of radicals and the NO_x present in the atmosphere.

This non-linear nature of the atmosphere must be taken into account when policymakers consider control strategies for O_3 concentrations. The difficulty is exacerbated by the fact that regions can alternate between these regimes depending on the season, time of day etc.

Moreover, an air parcel emitted in an urban area may also evolve as outlined in Figure 1.3, as it moves downwind. Once the air parcel has been emitted, it would typically fall into the VOC-sensitive regime but as the parcel ages it would move into the NO_x-sensitive regime. Reducing VOC and NO_x would reduce tropospheric O_3, whilst reducing VOC levels would only be effective during VOC-sensitive regimes and reducing NO_x levels is only effective in NO_x-sensitive regimes and can even increase O_3 concentrations (Sillman, 1999). This is due to the radical or NO_x removal pathways that may or may not promote O_3 production as discussed above.

1.2   Ozone Production Potential

The difficulty in applying uniform and successful emission control strategies due to the different regimes of the atmosphere has given rise to a more thorough investigation into the ozone production capabilities of different VOCs, also called the Ozone Production Potential (OPP) of the VOC in question. This potential can be calculated via modelling studies and has given rise to reactivity scales classifying the OPP of VOCs or classes of VOCs. The OPP of a VOC is dependent on the meteorological conditions, the reactivity of the VOC and the location of its emission. A wide range of such scales have been developed and are discussed below.

1.2.1   MIR and MOIR Incremental Reactivity Scales

(Carter, 1994) outlines three incremental reactivity scales, the Maximum Incremental Reactivity (MIR), Maximum Ozone Incremental Reactivty (MOIR) and Equal Benefit Incremental Reactivity (EBIR) scales. The incremental reactivity of a VOC is defined as the change in O_3 concentration caused when adding a small amount of the VOC in question to the emissions. Incremental reactivities are typically investigated through modelling studies although they can also be determined by means of airshed studies.

The VOC reactivity, mechanism pathways and the atmospheric regime into which it is emitted all influence the incremental reactivity value of the VOC. Hence, the total NO_x available is extremely important, as this determines the atmospheric regime present. For example, in VOC-sensitive regimes, the VOCs will have larger incremental reactivities than in a NO_x-sensitive regime.

The MIR scale is calculated by adjusting the NO_x levels so that the largest incremental reactivity was achieved for the individual VOC. The MOIR scale differs from the MIR as it is calculated using NO_x levels that give the maximum ozone concentration for the whole VOC mix. Whilst calculating the EBIR scale involves adjusting the NO_x inputs so that the effect on O_3 for a specific percentage change in VOC has the same effect of an equal percentange change in NO_x (Carter, 1994). The MOIR and EBIR scales are also shown in (Carter, 1994) to be practically equivalent when factoring in uncertainties during their calculation.

The MIR and MOIR scales are applicable to different regions due to their differences in NO_x concentrations. The MIR scale is applicable to places that have high transport emissions such as Los Angeles, as this implies an increased amount of NO_x in the atmosphere when compared with the amount of VOCs. In contrast, the MOIR scale is more relevant to areas that have higher VOC (biogenic or anthropogenic) emissions. However, both scales do not include transport or multi-day scenarios during their calculation and this may effect their applicability (Capps et al.,

2010).

1.2.2   Photochemical Ozone Creation Potential

The Photochemical Ozone Creation Potential (POCP) was introduced in (Derwent et al., 1996) and was used to calculate ozone production under the conditions applicable to northwestern Europe. This is in contrast to the MIR and MOIR which are both applicable to the US, due to the NO_x levels used for their calculations and that in Europe the transport of reactive species and multi-day photochemistry are more important. Hence, the POCP values are calculated over a five day period.

The POCP is calculated by increasing the amount of a VOC in a photochemical trajectory model and calculating the increase in O_3 concentration. This is then expressed as a percentage using the ozone increase due to the same amount in mass of ethene as reference. The increased time period in the model runs to calculate the POCP values showed that almost all VOC increase their ozone formation potential over time. The exceptions to this are the highly reactive VOC as they are completely oxidised during the initial emission phase (Derwent et al., 1996).

The calculation of the POCP was further refined in (Derwent et al., 1998) by using a more detailed chemical mechanism in the atmospheric model than that used in (Derwent et al., 1996) and by also studying the influence of different NO_x concentrations. The Master Chemical Mechanism (MCM) is used as this provides a lot of chemical detail in the reaction mechanisms of the VOCs.

The general trend of the POCP values did not change when using the MCM, however the individual values themselves were affected. The NO_x inputs were also adjusted in order to mirror planned changes in NO_x emission standards and to investigate the robustness of these planned policies if based on POCPs. Once again, the same general trend of the POCP values was noted, although there are some VOCs (e.g. 1,3-butadiene) whose reactivity changed drastically depending on the NO_x conditions (Derwent et al., 1998). This again demonstrates the importance of taking into consideration the different possible regimes in the atmosphere as described in Section 1.1.6.

The use of incremental reactivity scales has been used in regulatory control in some US cities (Luecken and Mebust, 2008), where the MIR has mainly been used for such purposes. Due to the assumptions made during the generation of the scale itself, such as the NO_x levels, it is not straightforward to extend the use of an incremental reactivity scale to a larger geographical area. Moreover, the incremental reactivity scales are typically calculated using a box-model which does not include such factors as meteorology and may not include effects of transported air masses that, as previously discussed, can all influence the amount of O_3 produced.

A VOC's direct or indirect impact on ozone production cannot be distinguished when using incremental reactivity scales. The direct impact is the incremental effect of both the extra VOC and the resulting oxidation intermediates. Whilst the indirect impact is the effect that these VOC increments have on the availability of radical species which in turn influences the ozone production from other compounds in the base VOC mixture (Butler et al., 2011), as discussed in Section 1.1.6. Another disadvantage is that the reactivity scales do not include detailed chemical information on the oxidation reactions of the VOC and how this is related to the OPP, moreover some scales do not account for the temporal effects of ozone production.

1.2.3   Tagged Ozone Production Potential

This led to a new approach outlined in (Butler et al., 2011) that links the degradation products of VOCs by using a tagging approach, called the Tagged Ozone Production Potential (TOPP). The calculation of the TOPP is taken over multiple days and calculates the direct impact of a particular VOC on its total impact on the O_x family, defined previously in Section 1.1.3. The TOPP was calculated for NMVOCs listed in Table 1.2 and the atmospheric conditions related to Los Angeles and Beijing and gave similar results despite these two cities having different NMVOC profiles.

The TOPP values also indicate two groups of NMVOCs, those that reach a maximum in the first day of the simulation followed by a decrease and those reaching a maximum TOPP after the first day. The first group includes many reactive NMVOCs such as alkenes and xylenes whilst the second group includes the slower reacting species such as alkanes and benzene. These groups can be determined as the time taken for a VOC to reach its maximum O_3 production potential is dependent on the rate at which VOCs yield smaller peroxy radical oxidation fragments.

(Butler et al., 2011) also compares the TOPP to the MIR, MOIR and POCP showing that the TOPP compares well with all three, although to differing degrees for different classes of NMVOCs in the cases of the MIR and MOIR. An added advantage of the tagging approach used for the TOPP calculations is that the reaction pathways of the VOC in question that contribute to O_3 production can be determined. As in (Butler et al., 2011), these reactions can be compared for different VOCs to determine the reactions that directly effect ozone production.

1.3   Atmospheric Chemical Transport Models

Predictions of future O_3 pollution levels are typically performed using mathematical atmospheric chemical transport models, these can be of different types

depending on the study being performed. What is common between models is that they all must include an emission inventory, transport of the species, atmospheric physical and chemical transformation and numerical solutions to the applicable differential equations.

Models are usually defined as either Eulerian or Lagrangian. The former describes the atmosphere in terms of fixed computational cells where species enter in and out of the cell walls and the concentrations of the species are then calculated as a function of time. Whilst the latter simulate changes of selected air parcels during advection through the atmosphere, hence there is no mass exchange between the surroundings and the air parcel (besides the emissions) and the model calculates concentrations at different locations at different times (Seinfeld and Pandis, 2006). Despite the differences that Eulerian and Langrangian models offer when undertaking a modelling study, Eulerian photochemical models constitute the majority of photochemical models (i.e. models dealing with atmospheric chemistry driven by photolysis as opposed to heterogeneous reactions) (Russell and Dennis, 2000).

Atmospheric models can also have different dimensions, ranging from zero-dimensional (also called a box model) to three-dimensional models. Box models have uniform atmospheric concentrations and are only a function of time, they are mainly used for focusing on the atmospheric chemistry or other detailed processes. Column models (or one-dimensional models) use concentrations that are a function of time and height, thus the grid is made up of many horizontally homogeneous layers. Two-dimensional models assume that concentration is constant in one direction and dependent on the other two directions and time. These models are used to describe global atmospheric chemistry with the assumption that concentration is a function of latitude and altitude but not longitude. Three-dimensional models calculate concentration as a function of all three directions and time. Accuracy, simplicity and use of computing power all increase with the dimension of the model (Seinfeld and Pandis, 2006).

The model inputs may include meteorology, atmospheric concentrations (also used for initial and boundary conditions), emissions, topography and the grid structure (Russell and Dennis, 2000). Some models include online calculations of these inputs at each time step. Boundary conditions are typically the most difficult initial condition to set accurately as this requires knowledge of the investigated species concentrations at the boundary edges (if applicable) of the model grid. The model's dimension and type determine the set of differential equations that will be solved at each time step of the model run. Numerical methods are then used to solve the differential equations with the specified initial and boundary conditions. These methods vary between models and may be Runge-Kutta (Sandu et al., 1997b), Finite Element (Russell and Dennis, 2000) or Rosenbrock methods (Sandu et al., 1997a), to name

three.

Setting the initial conditions involves fixing the starting concentrations of the species being studied, these conditions are dependent on the area being studied and whether it is an urban or rural area, amongst other considerations. The importance of setting the initial conditions depends on the model type, these conditions in Langrangian models are much more important than in Eulerian models, as this is the starting point at which the air parcel and its concentrations will be studied throughout the model run. Boundary conditions are concentration flows of species and are important for both Eulerian and Lagrangian models. Emission inventories of the studied area are typically used, this is also believed to be one of the more uncertain inputs in a modelling study (Russell and Dennis, 2000).

1.4   Chemical Mechanisms

Models use chemical mechanisms to implement the atmospheric chemistry at each time step during a model run. The mechanism includes rate coefficients, reaction pathways with the corresponding branching ratios, photolysis rates and reaction products, amongst other parameters. This part of a model consumes a great deal of the computing resources, hence, when using a three-dimensional model the mechanism will include less chemical detail compared to a study incorporating a box-model. To achieve this, mechanisms used primarily in three-dimensional models will aggregate compounds, include more assumptions about how reactions proceed and how the degradation products are treated when compared to mechanisms used in box-modelling studies.

The Master Chemical Mechanism (MCM) in (Saunders et al., 2003; Jenkin et al., 2003) is a near-explicit mechanism that is used for box modelling studies. Regional and global mechanisms include the Regional Atmospheric Chemistry Mechanism (RACM), the Carbon Bond Mechanism (CB-05 in (Yarwood et al., 2005)), the National Center for Atmospheric Research (NCAR) master mechanism ((Madronich and Calvert, 1989)) and the Statewide Air Pollution Research Center (SAPRC), although many mechanisms include reduced mechanisms that are applicable to different model dimensions. A brief discussion of these mechanisms are included in (Russell and Dennis, 2000) whilst the MCM, RACM and SAPRC mechanisms are discussed in more detail below.

1.4.1   Self-Generating Mechanisms

The self-generating mechanism is the type of chemical mechanism that reflects the details of the atmospheric chemistry summarised in Section 1.1 the most and

is also called an explicit mechanism. This requires thousands of reactions as the degradation of minor products is often more complex than that of the parent VOC. It also represents a compact method of obtaining a detailed mechanism that describes tropospheric chemistry.

(Aumont et al., 2005) outlines a way of including all reaction pathways that does not imply manually writing all the reactions with their respective parameters, as is the case for other mechanisms. This would also include the possibilty of heterogeneous chemistry and aerosol formation being accouted for in the mechanism, these are aspects of atmospheric chemistry that are not treated in great detail in chemical mechanisms used for gas-phase calculations.

The approach in (Aumont et al., 2005) is to write a so-called 'generator' program that analyses the chemical structure of the VOC being studied to determine the reactive sites which then give the reaction pathways. The generator then accesses another file which includes the available reaction parameters and the reaction products. Structure activity relationships (SARs) are used when no reaction parameters are available. A file is then created that contains the final reaction, it includes the reactants, products and rate coefficients amongst other information. This process is then repeated for the products until all the oxidation reactions have been completed.

There are a number of advantages of this type of mechanism over mechanisms that are manually written up reaction by reaction. Firstly, a self-generating mechanism is faster to write since there are less reactions that need to be written due to the use of a generator program. This also implies increased accuracy (less manually written reactions means less typographical errors) and also maintenance is much easier as far less code needs to be updated. Currently, this type of mechanism has not been used in relation to ozone production potential calculations.

1.4.2   Master Chemical Mechanism

The Master Chemical Mechanism (MCM) v3.2 is a near-explicit mechanism describing the chemical degradation of 107 non-aromatic VOCs in (Saunders et al., 2003) and 18 aromatic VOCs in (Jenkin et al., 2003). In total the MCM v3.2 has 12,691 reactions including 4351 organic compounds and 46 associated inorganic compounds. The MCM includes alkanes, alkenes, dienes, monoterpenes, aromatics, aldehydes and ketones amongst others, the complete list is found online (`http://mcm.leeds.ac.uk/MCM/`). The VOCs were chosen in accordance with the UK National Atmospheric Emissions Inventory and include those that make up about 70% of the mass emissions of unique species achieved.

Each primary VOC and each degradation product, is individually degraded until it is broken down to CO_2, CO or an organic product (or radical) already found in

the MCM (Jenkin et al., 1997). The main assumptions made to reduce the number of reactions and compounds in the MCM are given below and are taken from (Jenkin et al., 1997).

1. The number of product channels resulting from reaction with the OH radical is limited by disregarding those pathways of low probability.

2. Many permutation (i.e. self and cross) reactions of organic peroxy radicals are represented by a single parameterised reaction. This is particularly required as inclusion of all peroxy radical reactions would involve about 400,000 reactions.

3. The degradation chemistry is simplified, especially for those "side" products deemed to be minor.

Figure 1.4 shows the reaction pathways represented in the MCM of a primary VOC, these shall be summarised below. First the schemes used for the degradation reactions of non-aromatic VOCs in (Saunders et al., 2003) shall be discussed. As mentioned above, the main reaction pathway for VOC degradation is by OH radical reaction and hence this is included for the vast majority of VOCs considered. Reaction with O_3 is deemed to only be important for alkenes, dienes, monoterpenes and some unsaturated oxygenated products. Reaction with the NO_3 radical is mainly important during the night-time and for alkenes, dienes, aldehydes and ethers.

For all reactions in the MCM, rate coefficients are taken from literature, where available, if not then they are estimated using methods also described in literature (for example, via SAR and group reactivity (GR) methods). The branching ratios of all reactions are also taken or estimated from literature. The reactions with O_3 and the NO_3 radical are also included if the parent VOC has a rate of removal that is more than 1% of its removal rate with the OH radical and its lifetime with respect to reaction with O_3 (or NO_3, accordingly) is less than 10^7 seconds.

Photolysis is included for those compounds that absorb at wavelengths less than 290 nm. The photolysis parameters are given for those compounds for which absorption cross-sections and quantum yield data is known and they are also determined as a function of the solar zenith angle.

The degradation products are also treated in detail, these first generation products are also degraded further as part of the MCM. Those products that have significant tropospheric concentrations are already treated in the MCM. To simplify this part of the mechanism, the products are limited to their reaction pathways with the OH radical. Those products which are deemed as minor are also greatly simplified whilst retaining product lifetimes and maintaining the carbon and nitrogen balance. However, many of these reactions are unbalanced in their O_2 or H_2O output (Jenkin
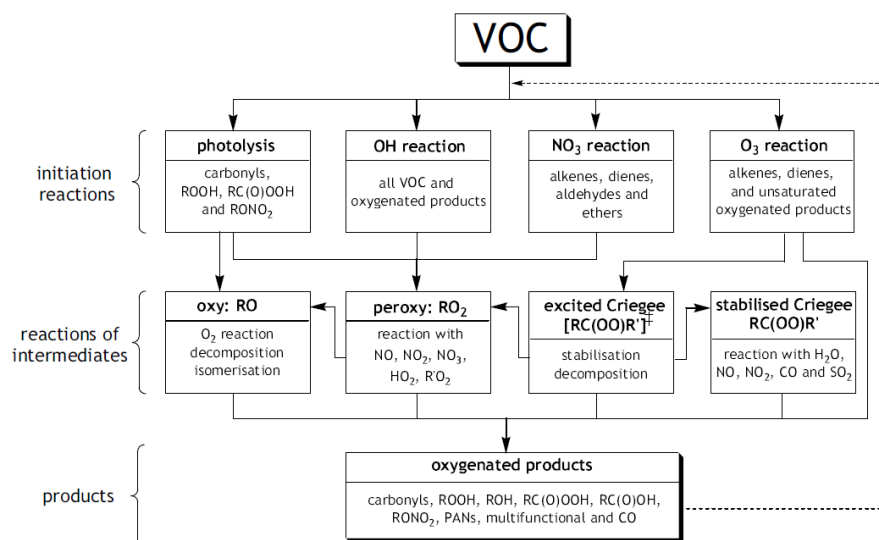
Figure 1.4: Flowchart of the major reactions, reactions of intermediates and products considered in the MCM. Taken from (Saunders et al., 2003)

et al., 1997). The kinetic data, where available, is taken from literature however mainly SAR estimations are used due to the lack of data.

In (Jenkin et al., 2003) the treatment of the aromatic VOCs included in the MCM v3.2 is described, this is summarised below. Where possible the treatment follows that of non-aromatic VOCs as outlined above and in (Saunders et al., 2003). However this is not possible for many reactions due to the intricacies of aromatic VOC chemistry and the fact that there is a lack of knowledge of the detailed degradation schemes. Also, similar simplifications are again present to reduce the complexity of the mechanism, this is particularly true for the C_6-C_{11} aromatic compounds.

Reaction with the OH radical is the main reaction pathway of aromatic compounds, the relevant rate coefficients are taken from literature, where available, or estimated depending on the functional group (Jenkin et al., 2003). The reaction pathways are known to proceed by H-atom abstraction or by addition to the aromatic ring. The branching ratios are taken from literature or applied from the analogous molecule for which there is information. H-atom abstraction is typically deemed to be a minor pathway, at this point the simplification applied is that only one pathway during the initial OH radical attack is chosen. Literature provides the data at which point in the aromatic ring the addition reaction occurs and also the following reaction with O_2. Some specific cases are treated separately according to the relevant literature (Jenkin et al., 2003).

The previous conditions outlined above for reaction with O_3 and with the NO_3 radical are also applied to aromatics VOCs. Again, all rate coefficients and branching ratios are either taken or estimated from the available data and the reaction pathways

also proceed as described in literature. Photolysis is only considered for some aromatic VOCs based on the conditions described above. For those cases in which data are not available, the photolysis rates are taken by extension of the data available (Jenkin et al., 2003). Hence, all reactions proceed as described in literature with estimations used for those cases lacking data.

The degradation products are also further degraded in the MCM, these are split into two general groups - those still containing an aromatic ring and those formed after ring-opening. The latter are then treated as non-aromatic compounds as described above in (Saunders et al., 2003). The former group is then further divided into four categories depending on the resulting product and these are then degraded according to (Jenkin et al., 2003).

### 1.4.3   Regional Atmospheric Chemistry Mechanism

Another chemical mechanism is the Regional Atmospheric Chemistry Mechanism (RACM), described in (Stockwell et al., 1997) and described below. This is a complete revision of the Regional Acid Deposition (RADM2) mechanism and is applicable to regional modelling and capable of simulating the gas phase tropospheric chemistry over remote and heavily polluted urban regions, including at the Earth's surface and in the upper troposphere. The RACM includes 17 inorganic, four inorganic intermediates and 32 organic species, four of which are of biogenic origin that altogether entail about 237 reactions. The inorganic reactions are practically fully described with the relevant rate coefficients, quantum yields and photolysis coefficients taken from literature.

In order to reduce computational resources for the mechanistic part of a regional model, the organic compounds are grouped into 16 anthropogenic and three biogenic model species. This grouping is based upon emission rates, functional group similarity and OH radical reactivity. Obtaining the final model species was done in two steps, first the hundreds of anthropogenic VOCs were grouped into 32 emission categories and then these were aggregated into the final 16 model species. Another aspect of reducing computational requirements was achieved by reducing the number of reaction pathways by only taking one reaction pathway from those available and also not treating all the organic intermediates explicitly.

The reaction rate coefficients of the model species are obtained by a weighted mean of all the rate coefficients of the organic species aggregated into the model species, this is done to account for the difference in reactivities between the model and chemical species. The individual rate coefficients are taken from literature or estimated by means of a SAR. Some organic compounds (for example, methane and ethene) are explicitly treated, if not then the compounds are represented by a model

species. For example, excluding ethene, anthropogenic alkenes with their double bond at the end of the molecule are included as the model species as OLT whilst anthropogenic alkenes with their double bond not at the end of the molecule are represented by OLI (Stockwell et al., 1997).

The different functional groups in a model species give rise to different reaction products, hence other model species are introduced with the relevant product yield fractions, as illustrated in the below reactions.

$$\text{OLT} + \text{OH} \longrightarrow \text{OLTP} \quad (\text{R31})$$
$$\text{OLI} + \text{OH} \longrightarrow \text{OLIP} \quad (\text{R32})$$
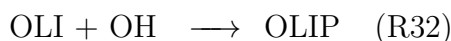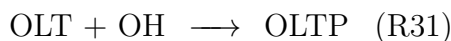
These product species are calculated as a weighted mean of the product yields of all the chemical species represented by the model species, where the individual yields are taken from literature.

The branching ratios of certain reactions are also parameterised, for example the slow-reacting aromatic species, represented by the model species TOL, are assumed to react with the OH radical by addition to the aromatic ring with a 0.1 fraction of the reactions proceeding by H-atom abstraction.

$$\text{TOL} + \text{OH} \longrightarrow 0.90 \text{ ADDT} + 0.10 \text{ XO}_2 + 0.10 \text{ HO}_2 \quad (\text{R33})$$
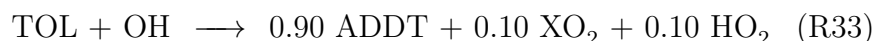
Furthermore, the branching ratios of the reactions of the aromatic-OH adduct (ADDT) are determined by simulating the environmental chamber data and this calculation is dependent on the secondary products formed from the reactions of unsaturated dicarbonyls. This is a source of uncertainity in the mechanism and since these three pathways after the O_3 production rate, obtaining the correct branching ratio is of importance (Stockwell et al., 1997).

The model species XO_2 is used to represent peroxy radicals where the appropriate XO_2 radical is dependent on the rate coefficient of the generating reaction. Also, the product yields are once again obtained via a weighted mean of the product yields of the individual species. To paramaterise the vast amount of reactions, very fast reactions are ignored and reactions with O_3 are estimated due to the lack of experimental data.

(Kirchner and Stockwell, 1996) details the treatment of organic peroxy radicals. The organic-peroxy radical-organic peroxy radical reactions are represented by reactions of the organic-peroxy radical with the two most important peroxy radicals (CH_3O_2 and $CH_3C(O)O_2$) and all other reactions with organic-peroxy radicals are ignored. The reaction rate coefficients of organic-peroxy radical self and cross reactions were estimated using the method described in (Kirchner and Stockwell, 1996). Experimental data is used for the rate coefficients of alkyl peroxy radicals reaction with NO.

1.5   Comparison of Chemical Mechanisms

Given the different chemical mechanisms and their differing approaches towards simplifying the complexities of atmospheric chemistry, there have been many comparative studies to determine the differences between calculation results obtained when performing the same modelling study but altering the mechanism. In (Dunker et al., 1984) four mechanisms that were used in atmospheric modelling studies were compared by means of atmospheric simulations of box, trajectory and grid modelling studies and also against chamber study results. The comparison parameters were plotted O_3, NO_2 and PAN isopleths as well as the time span required for the maximum one hour average O_3, NO_2 and PAN concentrations to be reached. The largest differences between the mechanisms were found during the box model study whereas the other simulations correlated well. It is also highlighted that differences in chemistry can be masked by the effects of the meteorology and other parameters not included in a box model.

A study of the chemical mechanisms used mainly for European regional studies are compared in (Gross and Stockwell, 2003). Here, a box model study with the three different mechanisms is used to generate the concentrations of O_3, NO, NO_2, OH radical, HO_2 radical and organic peroxy radicals RO_2. O_3 isopleth plots are also generated by performing the study over a range of NO_x and VOC concentrations. A common set of photolysis coefficients were used so that the results would mirror only differences in the chemistry, the study also accounted for both urban and rural conditions in separate model runs.

The results show that the greatest differences between these mechanisms are in the O_3, NO_2 and RO_2 radical concentrations. The differences in the O_3 concentrations are linked to the discrepancies between the NO_2 and RO_2 concentrations as these are reactions that lead to O_3 production or loss. This emphasises the importance of the treatment of organic peroxy radicals, which is typically one of the major areas of difference between chemical mechanisms. The rural study showed little difference in the comparison parameters whilst the urban study showed larger differences. This can be attributed to the complexity of the organic chemistry prevalent in urban areas. (Gross and Stockwell, 2003) recommends that many different urban scenarios be considered and that O_3 isopleth plots giving the O_3 concentration over a range of NO_x and VOC values should be used for such mechanism comparison studies.

(Emmerson and Evans, 2009) compares the gas-phase chemical mechanisms used in global models. Since the MCM contains more chemical details than the reduced schemes used in global models it is used as a reference to which these are compared. The comparison is performed by box model runs simulating a large number of scenarios that are characteristic of global situations - industrial, clean, cold and dry,

hot and wet, biogenic and non-biogenic conditions. Moreover, a particular recorded event (where the data are taken from the summer 2003 TORCH campaign) is also simulated with all the models to determine how close the simulation results are to the actual recorded concentrations.

The simulations were ran without heterogenous chemistry and all set to begin at midnight in order to investigate the effect of night-time chemistry, which would be affected most by not including heterogenous chemistry. The length of each simulation is five days as a compromise between very long and very short run times which can affect the chemistry in different ways. Long model runs would imply significant ageing of the air masses that would drive the chemistry and very short model runs would not test the chemistry pertaining to the degradation products at all, hence a compromise needs to be found. Separate model runs were also performed to determine differences in the inorganic chemistry, full chemistry and night-time chemistry.

The resulting concentrations of specific compounds were plotted and compared to verify where mechanistic differences arise. The little difference between inorganic chemistry regimes can be attributed to the differences between kinetic data supplied by IUPAC and JPL, whilst there are more differences between the full chemistry and night-time chemistry. The greatest differences in the organic chemistry is when biogenic compounds, such as isoprene, are considered and are present in larger concentrations. For the specific pollution event that was modelled, the greatest differences arise for the night-time chemistry and O_3 concentrations.

Reactivity scales have also been used as comparison tool for chemical mechanisms, this was proposed as in a single number, they provide a lot chemical kinetic data. In (Derwent et al., 2010), the MCM and SAPRC are compared by calculation of the POCP of 116 organic compounds from the major atmospheric classes within both mechanisms. A series of photochemical trajectory model runs simulating a single day were performed, many parameters other than the mechanisms were adjusted as incremental reactivities are not solely geophysical measures but rely on many other parameters.

The MCM and the SAPRC were chosen for this study as they are near-explicit mechanisms with the main difference being in how they treat the first generation products - the MCM continues in an explicit manner while the SAPRC uses aggregation techniques. In general, the POCP values correlate very well between the two mechanisms, with a small number of exceptions. These can be attributed to the lack of detailed understanding of the degradation reactions of these compounds. The good correlation of reactivities of the aromatic compounds merely indicates that both mechanisms treat aromatic compounds similarly rather than having a detailed knowledge of these degradation schemes.

A detailed look at the chemistry affecting different mechanisms used in air

quality modelling is described in (Stockwell et al., 2012), where a box modelling study is undertaken with near-explicit and aggregated chemical mechanisms. The model system used is the same as that used in (Seefeld and Stockwell, 1999) with only gas-phase chemistry and constant meteorological conditions. Different model runs were also undertaken with different temperatures in order to determine the temperature dependency of model results.

The study highlights that the temperature dependence of gas phase reactions is uncertain for both organic and inorganic compounds. Also, night-time chemistry is a major source of uncertainty. Other knowledge gaps include the rate coefficients of the reactions of organic peroxy radicals as well as the products resulting from these reactions, the detailed degradation of both aromatic and biogenic compounds.

Chapter 2

Methodology

Chapter 3

Presentation of Papers

This chapter will outline the main findings in each of the scientific papers that were published as part of the PhD.

3.1 Paper 1: A comparison of chemical mechanisms using tagged ozone production potential (TOPP) analysis

The first paper described a box modelling study in which the secondary chemistry represented in many reduced chemical mechanisms (Table) for VOC typical of urban environments (Table 2 of the article) were compared to the detailed MCM chemical mechanisms. The research question addressed in this paper was to verify whether these different representations of this secondary chemistry influence ozone production.

The degradation of each VOC prescribed in each chemical mechanism was "tagged" so that the O_x production, a proxy for O_3 production, could be attributed to the individual VOC sources. Tagging the chemical mechanisms involved labelling every organic degradation product from a VOC with the name of the emitted VOC, thus each VOC has a separate set of reactions fully describing its degradation until the final products, CO_2 and H_2O, are produced.

The ozone mixing ratios from reduced chemical mechanisms were generally lower than the mixing ratios from the reference MCM chemical mechanisms on the first two days of the simulations. The VOC degradation prescribed in CRI v2, a lumped-intermediate mechanism, produced the most similar amounts of O_x to the

MCM v3.2 for each VOC. Thus, the approach of using lumped-intermediate species whose degradation are based upon more detailed chemical mechanisms is preferable when developing future chemical mechanisms.

Many VOC are broken down into smaller-sized degradation products faster on the first day in reduced chemical mechanisms than the MCM v3.2 leading to lower amounts of larger-sized degradation products that can further degrade and produce O_x. Thus, many VOC in reduced chemical mechanisms produce a lower maximum of O_x than the MCM v3.2 ultimately leading to lower O_3 mixing ratios from the reduced chemical mechanisms compared to the MCM v3.2.

Reactive VOC, such as unsaturated aliphatic and aromatic VOC, produce maximum O_x on the first day of the simulations. Unsaturated aliphatic VOC produce similar amounts of O_x on the first day between mechanisms; differences in O_x production arise when mechanism species are used to represent individual VOC. Large inter-mechanism differences in O_x production result from the degradation of aromatic VOC on the first day due to the faster break down of the mechanism species representing aromatic VOC in reduced chemical mechanisms.

The less-reactive alkanes produce maximum O_x on the second day of simulations and this maximum is lower in each reduced chemical mechanism than the MCM v3.2 due to the faster break down of alkanes into smaller sized degradation products on the first day. The lower maximum in O_x production during alkane degradation in reduced mechanisms would lead to an underestimation of the O_3 levels downwind of VOC emissions, and an underestimation of the VOC contribution to tropospheric background O_3 when using reduced mechanisms in regional or global modelling studies.

3.2   Paper 2:

3.3   Paper 3:

Chapter 4

Overall Discussion and Conclusions

Chapter 5

Summary and Zusammenfassung

References

Christof Appenzeller, James R. Holton, and Karen H. Rosenlof. Seasonal variation of mass transport across the tropopause. *Journal of Geophysical Research*, 101(D10): 15,071–15,078, 1996.

C. Arsene, A. Bougiatioti, and N. Mihalopoulos. Sources and variability of non-methane hydrocarbons in the Eastern Mediterranean. *Global NEST Journal*, 11 (3):333–340, 2009.

Roger Atkinson. Gas phase tropospheric chemistry of organic compounds: a review. *Atmospheric Environment*, 24A(1):1–41, 1990.

Roger Atkinson. Atmospheric chemistry of VOCs and NO_x. *Atmospheric Environment*, 34(12-14):2063–2101, 2000.

B. Aumont, S. Szopa, and S. Madronich. Modelling the evolution of organic carbon during its gas-phase tropospheric oxidation: Development of an explicit model based on a self generating approach. *Atmospheric Chemistry and Physics*, 5(9):2497–2517, 2005.

Angela K. Baker, Andreas J. Beyersdorf, Lambert A. Doezema, Aaron Katzenstein, Simone Meinardi, Isobel J. Simpson, Donald R. Blake, and F. Sherwood Rowland. Measurements of nonmethane hydrocarbons in 28 United States cities. *Atmospheric Environment*, 42:170–182, 2008.

Agnès Borbon, Hervè Fontaine, Nadine Locoge, Marc Veillerot, and J. C. Galloo. Developing receptor-oriented methods for non-methane hydrocarbon characterisation in urban air - Part I: source identification. *Atmospheric Environment*, 37:4051–4064, 2003.

A. W. Brewer. Evidence of a world circulation provided by the measurements of helium and water vapour distribution in the stratosphere. *Quarterly Journal of the Royal Meteorological Society*, 75(326):351–363, 1949.

T. M. Butler, M. G. Lawrence, D. Taraborrelli, and J. Lelieveld. Multi-day ozone production potential of volatile organic compounds calculated with a tagging approach. *Atmospheric Environment*, 45(24):4082–4090, 2011.

Shannon L. Capps, Yongtao Hu, and Armistead G. Russell. Assessing Near-Field and Downwind Impacts of Reactivity-Based Substitutions. *Journal of the Air and Waste Management Association*, 60:316–327, 2010.

William P. L. Carter. Development of Ozone Reactivity Scales for Volatile Organic Compounds. *Journal of the Air and Waste Management Association*, 44:881–899, 1994.

J. Coates and T. M. Butler. A comparison of chemical mechanisms using tagged ozone production potential (TOPP) analysis. *Atmospheric Chemistry and Physics*, 15(15):8795–8808, 2015.

R. G. Derwent, M. E. Jenkin, and S. M. Saunders. Photochemical Ozone Creation Potentials for a Large Number of Reactive Hydrocarbons under European Conditions. *Atmospheric Environment*, 30(2):181–199, 1996.

Richard G. Derwent, Michael E. Jenkin, Sandra M. Saunders, and Michael J. Pilling. Photochemical Ozone Creation Potentials for Organic Compounds in Northwest Europe Calculated with a Master Chemical Mechanism. *Atmospheric Environment*, 32(14/15):2429–2441, 1998.

Richard G. Derwent, Michael E. Jenkin, Michael J. Pilling, William P. L. Carter, and Ajith Kaduwela. Reactivity Scales as Comparative Tools for Chemical Mechanisms. *Journal of the Air and Waste Management Association*, 60:914–924, 2010.

G. B. M. Dobson. Origin and distribution of polyatomic molecules in the atmosphere. *Proceedings of the Royal Society London A*, 236(1205):187–193, 1956.

Alan M. Dunker, Sudarshan Kumar, and Peteris H. Berzins. A Comparison of Chemical Mechanisms Used In Atmospheric Models. *Atmospheric Environment*, 18 (2):311–321, 1984.

K. M. Emmerson and M. J. Evans. Comparison of tropospheric gas-phase chemistry schemes for use within global models. *Atmospheric Chemistry and Physics*, 9: 1831–1845, 2009.

Arlene M. Fiore, Daniel J. Jacob, Jennifer A. Logan, and Jeffrey H. Yin. Long-term trends in ground level ozone over the contiguous United States, 1980-1995. *Journal of Geophysical Research*, 103(D1):1471–1480, 1998.

A. H. Goldstein and I. E. Galbally. Known and unexplored organic constituents in the Earth's atmosphere. *Environmental Science and Technology*, 41(5):1514–1521, 2007.

Allan Gross and William R. Stockwell. Comparison of the EMEP, RADM2 and RACM Mechanisms. *Journal of Atmospheric Chemistry*, 44:151–170, 2003.

P. H. Haynes, C. J. Marks, M. E. McIntyre, T. G. Shephard, and K. P. Shine. On the "Downward Control" of Extratropical Diabatic Circulations by Eddy-Induced Mean Zonal Forces. *Journal of the Atmospheric Sciences*, 48(4):651–687, 1991.

P. Hess and N. Mahowald. Interannual variability in hindcasts of atmospheric chemistry: the role of meteorology. *Atmospheric Chemistry and Physics*, 9:5261–5280, 2009.

M. E. Jenkin, S. M. Saunders, V. Wagner, and M. J. Pilling. Protocol for the development of the Master Chemical Mechanism, MCM v3 (Part B): Tropospheric degradation of aromatic volatile organic compounds. *Atmospheric Chemistry and Physics*, 3(1):181–193, 2003.

Michael E. Jenkin and Kevin C. Clemitshaw. Ozone and other secondary photochemical pollutants: Chemical processes governing their formation in the planetary boundary layer. *Atmospheric Environment*, 34(16):2499–2527, 2000.

Michael E. Jenkin, Sandra M. Saunders, and Michael J. Pilling. The tropospheric degradation of volatile organic compounds: A protocol for mechanism development. *Atmospheric Environment*, 31(1):81–104, 1997.

Frank Kirchner and William R. Stockwell. Effect of peroxy radical reactions on the predicted concentrations of ozone, nitrogenous compounds and radicals. *Journal of Geophysical Research*, 101(D15):21,007–21,002, 1996.

Frank Kirchner, Francois Jenneret, Alain Clappier, Bernd Krüger, Hubert van den Bergh, and Bertrand Calpini. Total VOC reactivity in the planetary boundary layer 2. A new indicator for determining the sensitivity of the ozone production to VOC and NO_x. *Journal of Geophysical Research*, 106(D3):3095–3110, 2001.

Lawrence I. Kleinman. Seasonal Dependence of Boundary Layer Peroxide Concentration: The Low and High NO_x Regimes. *Journal of Geophysical Research*, 96(D11):20,721–20,733, 1991.

Lawrence I. Kleinman. Low and high NO_x tropospheric photochemistry. *Journal of Geophysical Research*, 99(D8):16,831–16,838, 1994.

L.I. Kleinman. The dependence of tropospheric ozone production rate on ozone precursors. *Atmospheric Environment*, 39(3):575–586, 2005.

J.-H. Koo, Y. Wang, T. P. Kurosu, K. Chance, A. Rozanov, A. Richter, S. J. Oltmans, A. M. Thompson, J. W. Hair, M. A. Fenn, A. J. Weinheimer, T. B. Ryerson, S. Solberg, L. G. Huey, J. Liao, J. E. Dibb, J. A. Neuman, J. B. Nowak, R. B. Pierce, M. Natarajan, and J. Al-Saadi. Characteristics of tropospheric ozone depletion events in the Arctic spring: analysis of the ARCTAS, ARCPAC, and ARCIONS measurements and satellite BrO observations. *Atmospheric Chemistry and Physics*, 12:9909–9922, 2012.

Jos Lelieveld and Frank J. Dentener. What controls tropospheric ozone? *Journal of Geophysical Research*, 105(D3):3531–3551, 2000.

C.-Y. Cynthia Lin, Daniel J. Jacob, and Arlene M. Fiore. Trends in exceedances of the ozone air quality standard in the continental United States, 1980-1998. *Atmospheric Environment*, 35:3217–3228, 2001.

D. J. Luecken and M. R. Mebust. Technical Challenges Involved in Implementation of VOC Reactivity-Based Control of Ozone. *Environmental Science and Technology*, 42(5):1615–1622, 2008.

Sasha Madronich and Jack G. Calvert. The NCAR Master Mechanism of the Gas Phase Chemistry - Version 2.0. Technical report, National Center of Atmospheric Research, 1989.

W. J. Moxim, W. Levy II, and P. S. Kasibhatla. Simulated global tropospheric PAN: Its transport and impact on NO_x. *Journal of Geophysical Research*, 101(D7): 12,621–12,638, 1996.

S. A. Penkett and K. A. Brice. The spring maximum of photo-oxidants in the Northern Hemisphere troposphere. *Nature*, 319:655–657, 1986.

Armistead Russell and Robin Dennis. NARSTO critical review of photochemical models and modeling. *Atmospheric Environment*, 34:2283–2324, 2000.

A. Sandu, J. G. Verwer, J. G. Blom, E. J. Spee, G. R. Carmichael, and F. A. Potra. Benchmarking stiff ODE solvers for atmospheric chemistry problems II: Rosenbrock solvers. *Atmospheric Environment*, 31(20):3459–3472, 1997a.

A. Sandu, J. G. Verwer, M Van Loon, G. R. Carmichael, F. A. Potra, D. Dabdub, and J. H. Seinfeld. Benchmarking stiff ODE solvers for atmospheric chemistry problems I: implicit vs explicit. *Atmospheric Environment*, 31(19):3151–3166, 1997b.

S. M. Saunders, M. E. Jenkin, R. G. Derwent, and M. J. Pilling. Protocol for the development of the Master Chemical Mechanism, MCM v3 (Part A): Tropospheric degradation of non-aromatic volatile organic compounds. *Atmospheric Chemistry and Physics*, 3(1):161–180, 2003.

S. Seefeld and W.R. Stockwell. First-order sensitivity analysis of models with time-dependent parameters: An application to PAN and ozone. *Atmospheric Environment*, 33(18):2941–2953, 1999.

John H. Seinfeld and Spyros N. Pandis. *Atmospheric Chemistry and Physics: From Air Pollution to Climate Change*. John Wiley & Sons Inc, 2 edition, 2006. ISBN 978-0-471-72018-8.

Sanford Sillman. The relation between ozone, NO_x and hydrocarbons in urban and polluted rural environments. *Atmospheric Environment*, 33(12):1821–1845, 1999.

William R. Stockwell, Frank Kirchner, Michael Kuhn, and Stephan Seefeld. A new mechanism for regional atmospheric chemistry modeling. *Journal of Geophysical Research D: Atmospheres*, 102(22):25,847–25,879, 1997.

William R. Stockwell, Charlene V. Lawson, Emily Saunders, and Wendy S. Goliff. A Review of Tropospheric Atmospheric Chemistry and Gas-Phase Chemical Mechanisms for Air Quality Modeling. *Atmosphere*, 3:1–32, 2012.

Kengo Sudo and Masaaki Takashi. Simulation of tropospheric ozone changes during 1997-1998 El Niño: Meteorological impact on tropospheric photochemistry. *Geophysical Research Letters*, 28(21):4091–4094, 2001.

World Meteorological Organisation. Scientific Assessment of Ozone Depletion: 2010. Technical Report 516 pp., World Meteorological Organisation, Geneva, Switzerland, March 2011.

Greg Yarwood, Sunja Rao, Mark Yocke, and Gary Z. Whitten. Updates to the Carbon Bond Chemical Mechanism: CB05. Technical report, U. S Environmental Protection Agency, 2005.

Chapter 6

Paper 1: A comparison of chemical mechanisms using tagged ozone production potential (TOPP) analysis

**Atmospheric
Chemistry
and Physics**

A comparison of chemical mechanisms using tagged ozone production potential (TOPP) analysis

J. Coates and T. M. Butler

Institute for Advanced Sustainability Studies, Potsdam, Germany

Correspondence to: J. Coates (jane.coates@iass-potsdam.de)

Abstract. Ground-level ozone is a secondary pollutant produced photochemically from reactions of NO_x with peroxy radicals produced during volatile organic compound (VOC) degradation. Chemical transport models use simplified representations of this complex gas-phase chemistry to predict O_3 levels and inform emission control strategies. Accurate representation of O_3 production chemistry is vital for effective prediction. In this study, VOC degradation chemistry in simplified mechanisms is compared to that in the near-explicit Master Chemical Mechanism (MCM) using a box model and by "tagging" all organic degradation products over multi-day runs, thus calculating the tagged ozone production potential (TOPP) for a selection of VOCs representative of urban air masses. Simplified mechanisms that aggregate VOC degradation products instead of aggregating emitted VOCs produce comparable amounts of O_3 from VOC degradation to the MCM. First-day TOPP values are similar across mechanisms for most VOCs, with larger discrepancies arising over the course of the model run. Aromatic and unsaturated aliphatic VOCs have the largest inter-mechanism differences on the first day, while alkanes show largest differences on the second day. Simplified mechanisms break VOCs down into smaller-sized degradation products on the first day faster than the MCM, impacting the total amount of O_3 produced on subsequent days due to secondary chemistry.

1   Introduction

Ground-level ozone (O_3) is both an air pollutant and a climate forcer that is detrimental to human health and crop growth (Stevenson et al., 2013). O_3 is produced from the reactions of volatile organic compounds (VOCs) and nitro-

gen oxides ($NO_x = NO + NO_2$) in the presence of sunlight (Atkinson, 2000).

Background O_3 concentrations have increased during the last several decades due to the increase of overall global anthropogenic emissions of O_3 precursors (HTAP, 2010). Despite decreases in emissions of O_3 precursors over Europe since 1990, EEA (2014) reports that 98 % of Europe's urban population are exposed to levels exceeding the WHO air quality guideline of $100\,\mu g\,m^{-3}$ over an 8 h mean. These exceedances result from local and regional O_3 precursor gas emissions, their intercontinental transport and the non-linear relationship of O_3 concentrations to NO_x and VOC levels (EEA, 2014).

Effective strategies for emission reductions rely on accurate predictions of O_3 concentrations using chemical transport models (CTMs). These predictions require adequate representation of gas-phase chemistry in the chemical mechanism used by the CTM. For reasons of computational efficiency, the chemical mechanisms used by global and regional CTMs must be simpler than the nearly explicit mechanisms which can be used in box modelling studies. This study compares the impacts of different simplification approaches of chemical mechanisms on O_3 production chemistry focusing on the role of VOC degradation products.

$$NO + O_3 \rightarrow NO_2 + O_2 \tag{R1}$$
$$NO_2 + h\nu \rightarrow NO + O(^3P) \tag{R2}$$
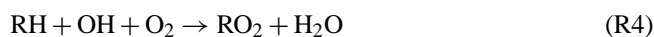$$O_2 + O(^3P) + M \rightarrow O_3 + M \tag{R3}$$

The photochemical cycle (Reactions R1–R3) rapidly produces and destroys O_3. NO and NO_2 reach a near-steady state via Reactions (R1) and (R2) which is disturbed in two cases. Firstly, via O_3 removal (deposition or Reaction R1 during night-time and near large NO sources) and secondly,

when O_3 is produced through VOC–NO_x chemistry (Sillman, 1999).

VOCs (RH) are mainly oxidised in the troposphere by the hydroxyl radical (OH) forming peroxy radicals (RO_2) in the presence of O_2. For example, Reaction (R4) describes the OH oxidation of alkanes proceeding though abstraction of an H from the alkane. In high-NO_x conditions, typical of urban environments, RO_2 react with NO (Reaction R5) to form alkoxy radicals (RO), which react quickly with O_2 (Reaction R6) producing a hydroperoxy radical (HO_2) and a carbonyl species (R′CHO). The secondary chemistry of these first-generation carbon-containing oxidation products is analogous to the sequence of Reactions (R4–R6), producing further HO_2 and RO_2 radicals. Subsequent-generation oxidation products can continue to react, producing HO_2 and RO_2 until they have been completely oxidised to CO_2 and H_2O. Both RO_2 and HO_2 react with NO to produce NO_2 (Reactions R5 and R7) leading to O_3 production via Reactions (R2) and (R3). Thus, the amount of O_3 produced from VOC degradation is related to the number of NO to NO_2 conversions by RO_2 and HO_2 radicals formed during VOC degradation (Atkinson, 2000).

$$RH + OH + O_2 \rightarrow RO_2 + H_2O \qquad (R4)$$

$$RO_2 + NO \rightarrow RO + NO_2 \qquad (R5)$$

$$RO + O_2 \rightarrow R'CHO + HO_2 \qquad (R6)$$

$$HO_2 + NO \rightarrow OH + NO_2 \qquad (R7)$$

Three atmospheric regimes with respect to O_3 production can be defined (Jenkin and Clemitshaw, 2000). In the NO_x-sensitive regime, VOC concentrations are much higher than those of NO_x, and O_3 production depends on NO_x concentrations. On the other hand, when NO_x concentrations are much higher than those of VOCs (VOC-sensitive regime), VOC concentrations determine the amount of O_3 produced. Finally, the NO_x–VOC-sensitive regime produces maximal O_3 and is controlled by both VOC and NO_x concentrations.

These atmospheric regimes remove radicals through distinct mechanisms (Kleinman, 1991). In the NO_x-sensitive regime, radical concentrations are high relative to NO_x leading to radical removal by radical combination (Reaction R8) and bimolecular destruction (Reaction R9) (Kleinman, 1994).

$$RO_2 + HO_2 \rightarrow ROOH + O_2 \qquad (R8)$$

$$HO_2 + OH \rightarrow H_2O + O_2 \qquad (R9)$$

However, in the VOC-sensitive regime, radicals are removed by reacting with NO_2 leading to nitric acid (HNO_3) (Reaction R10) and PAN species (Reaction R11).

$$NO_2 + OH \rightarrow HNO_3 \qquad (R10)$$

$$RC(O)O_2 + NO_2 \rightarrow RC(O)O_2NO_2 \qquad (R11)$$
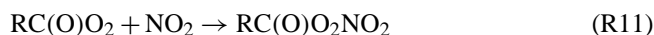
The NO_x–VOC-sensitive regime has no dominant radical removal mechanism as radical and NO_x amounts are comparable. This chemistry results in O_3 concentrations being a nonlinear function of NO_x and VOC concentrations.

Individual VOCs impact O_3 production differently through their diverse reaction rates and degradation pathways. These impacts can be quantified using ozone production potentials (OPPs), which can be calculated through incremental reactivity (IR) studies using photochemical models. In IR studies, VOC concentrations are changed by a known increment and the change in O_3 production is compared to that of a standard VOC mixture. Examples of IR scales are the maximum incremental reactivity (MIR) and maximum ozone incremental reactivity (MOIR) scales in Carter (1994), as well as the photochemical ozone creation potential (POCP) scale of Derwent et al. (1996, 1998). The MIR, MOIR and POCP scales were calculated under different NO_x conditions, thus calculating OPPs in different atmospheric regimes.

Butler et al. (2011) calculate the maximum potential of a number of VOCs to produce O_3 by using NO_x conditions inducing NO_x–VOC-sensitive chemistry over multi-day scenarios using a "tagging" approach – the tagged ozone production potential (TOPP). Tagging involves labelling all organic degradation products produced during VOC degradation with the name of the emitted VOCs. Tagging enables the attribution of O_3 production from VOC degradation products back to the emitted VOCs, thus providing detailed insight into VOC degradation chemistry. Butler et al. (2011), using a near-explicit chemical mechanism, showed that some VOCs, such as alkanes, produce maximum O_3 on the second day of the model run; in contrast to unsaturated aliphatic and aromatic VOCs which produce maximum O_3 on the first day. In this study, the tagging approach of Butler et al. (2011) is applied to several chemical mechanisms of reduced complexity, using conditions of maximum O_3 production (NO_x–VOC-sensitive regime), to compare the effects of different representations of VOC degradation chemistry on O_3 production in the different chemical mechanisms.

A near-explicit mechanism, such as the Master Chemical Mechanism (MCM) (Jenkin et al., 2003; Saunders et al., 2003; Bloss et al., 2005), includes detailed degradation chemistry making the MCM ideal as a reference for comparing chemical mechanisms. Reduced mechanisms generally take two approaches to simplifying the representation of VOC degradation chemistry: lumped-structure approaches and lumped-molecule approaches (Dodge, 2000).

Lumped-structure mechanisms speciate VOCs by the carbon bonds of the emitted VOCs (e.g. the Carbon Bond mechanisms, CBM-IV (Gery et al., 1989) and CB05 (Yarwood et al., 2005)). Lumped-molecule mechanisms represent VOCs explicitly or by aggregating (lumping) many VOCs into a single mechanism species. Mechanism species may lump VOCs by functionality (MODel for Ozone and Related chemical Tracers, MOZART-4, Emmons et al., 2010) or OH reactivity (Regional Acid Deposition Model, RADM2 (Stockwell et al., 1990), Regional Atmospheric Chemistry

Mechanism, RACM (Stockwell et al., 1997) and RACM2 (Goliff et al., 2013)). The Common Representative Intermediates mechanism (CRI) lumps the degradation products of VOCs rather than the emitted VOCs (Jenkin et al., 2008).

Many comparison studies of chemical mechanisms consider modelled time series of O_3 concentrations over varying VOC and NO_x concentrations. Examples are Dunker et al. (1984), Kuhn et al. (1998) and Emmerson and Evans (2009). The largest discrepancies between the time series of O_3 concentrations in different mechanisms from these studies arise when modelling urban rather than rural conditions and are attributed to the treatment of radical production, organic nitrate and night-time chemistry. Emmerson and Evans (2009) also compare the inorganic gas-phase chemistry of different chemical mechanisms; differences in inorganic chemistry arise from inconsistencies between IUPAC and JPL reaction rate constants.

Mechanisms have also been compared using OPP scales. OPPs are a useful comparison tool as they relate O_3 production to a single value. Derwent et al. (2010) compared the near-explicit MCM v3.1 and SAPRC-07 mechanisms using first-day POCP values calculated under VOC-sensitive conditions. The POCP values were comparable between the mechanisms. Butler et al. (2011) compared first-day TOPP values to the corresponding published MIR, MOIR and POCP values. TOPP values were most comparable to MOIR and POCP values due to the similarity of the chemical regimes used in their calculation.

In this study, we compare TOPP values of VOCs using a number of mechanisms to those calculated with the MCM v3.2, under standardised conditions which maximise O_3 production. Differences in O_3 production are explained by the differing treatments of secondary VOC degradation in these mechanisms.

2 Methodology

2.1 Chemical mechanisms

The nine chemical mechanisms compared in this study are outlined in Table 1 with a brief summary below. We used a subset of each chemical mechanism containing all the reactions needed to fully describe the degradation of the VOCs in Table 2. The reduced mechanisms in this study were chosen as they are commonly used in 3-D models and apply different approaches to representing secondary VOC chemistry. The recent review by Baklanov et al. (2014) shows that each chemical mechanism used in this study are actively used by modelling groups.

The MCM (Jenkin et al., 1997, 2003; Saunders et al., 2003; Bloss et al., 2005; Rickard et al., 2015) is a near-explicit mechanism which describes the degradation of 125 primary VOCs. The MCM v3.2 is the reference mechanism in this study due to its level of detail (16 349 organic reac-

tions). Despite this level of detail, the MCM had difficulties in reproducing the results of chamber study experiments involving aromatic VOCs (Bloss et al., 2005).

The CRI (Jenkin et al., 2008) is a reduced chemical mechanism with 1145 organic reactions describing the oxidation of the same primary VOCs as the MCM v3.1 (12 691 organic reactions). VOC degradation in the CRI is simplified by lumping the degradation products of many VOCs into mechanism species whose overall O_3 production reflects that of the MCM v3.1. The CRI v2 is available in more than one reduced variant, described in Watson et al. (2008). We used a subset of the full version of the CRI v2 (http://mcm.leeds.ac.uk/CRI). Differences in O_3 production between the CRI v2 and MCM v3.2 may be due to changes in the MCM versions rather than the CRI reduction techniques, hence the MCM v3.1 is also included in this study.

MOZART-4 represents global tropospheric and stratospheric chemistry (Emmons et al., 2010). Explicit species exist for methane, ethane, propane, ethene, propene, isoprene and α-pinene. All other VOCs are represented by lumped species determined by the functionality of the VOCs. Tropospheric chemistry is described by 145 organic reactions in MOZART-4.

RADM2 (Stockwell et al., 1990) describes regional-scale atmospheric chemistry using 145 organic reactions with explicit species representing methane, ethane, ethene and isoprene. All other VOCs are assigned to lumped species based on OH reactivity and molecular weight. RADM2 was updated to RACM (Stockwell et al., 1997) with more explicit and lumped species representing VOCs as well as revised chemistry (193 organic reactions). RACM2 is the updated RACM version (Goliff et al., 2013) with substantial updates to the chemistry, including more lumped and explicit species representing emitted VOCs (315 organic reactions).

CBM-IV (Gery et al., 1989) uses 46 organic reactions to simulate polluted urban conditions and represents ethene, formaldehyde and isoprene explicitly while all other emitted VOCs are lumped by their carbon bond types. All primary VOCs were assigned to lumped species in CBM-IV as described in Hogo and Gery (1989). For example, the mechanism species PAR represents the C–C bond. Pentane, having five carbon atoms, is represented as 5 PAR. A pentane mixing ratio of 1200 pptv is assigned to 6000 ($= 1200 \times 5$) pptv of PAR in CBM-IV. CBM-IV was updated to CB05 (Yarwood et al., 2005) by including further explicit species representing methane, ethane and acetaldehyde, and has 99 organic reactions. Other updates include revised allocation of primary VOCs and updated rate constants.

2.2 Model set-up

The modelling approach and set-up follows the original TOPP study of Butler et al. (2011). The approach is summarised here; further details can be found in the Supplement and in Butler et al. (2011). We use the MECCA box model,

Table 1. The chemical mechanisms used in the study are shown here. MCM v3.2 is the reference mechanism. The number of organic species and reactions needed to fully oxidise the VOCs in Table 2 for each mechanism are also included.

Chemical mechanism	Number of organic species	Number of organic reactions	Type of lumping	Reference	Recent study
MCM v3.2	1884	5621	No lumping	Rickard et al. (2015)	Koss et al. (2015)
MCM v3.1	1677	4862	No lumping	Jenkin et al. (1997) Saunders et al. (2003) Jenkin et al. (2003) Bloss et al. (2005)	Lidster et al. (2014)
CRI v2	189	559	Lumped intermediates	Jenkin et al. (2008)	Derwent et al. (2015)
MOZART-4	61	135	Lumped molecule	Emmons et al. (2010)	Hou et al. (2015)
RADM2	42	105	Lumped molecule	Stockwell et al. (1990)	Li et al. (2014)
RACM	51	152	Lumped molecule	Stockwell et al. (1997)	Ahmadov et al. (2015)
RACM2	92	244	Lumped molecule	Goliff et al. (2013)	Goliff et. al. (2015)
CBM-IV	19	47	Lumped structure	Gery et al. (1989)	Foster et al. (2014)
CB05	33	86	Lumped structure	Yarwood et al. (2005)	Dunker et al. (2015)

originally described by Sander et al. (2005), and as subsequently modified by Butler et al. (2011) to include MCM chemistry. In this study, the model is run under conditions representative of 34° N at the equinox (broadly representative of the city of Los Angeles, USA).

Maximum O_3 production is achieved in each model run by balancing the chemical source of radicals and NO_x at each time step by emitting the appropriate amount of NO. These NO_x conditions induce NO_x–VOC-sensitive chemistry. Ambient NO_x conditions are not required as this study calculates the maximum potential of VOCs to produce O_3. Future work should verify the extent to which the maximum potential of VOCs to produce O_3 is reached under ambient NO_x conditions.

VOCs typical of Los Angeles and their initial mixing ratios are taken from Baker et al. (2008), listed in Table 2. Following Butler et al. (2011), the associated emissions required to keep the initial mixing ratios of each VOC constant until noon of the first day were determined for the MCM v3.2. These emissions are subsequently used for each mechanism, ensuring the amount of each VOC emitted was the same in every model run. Methane (CH_4) was fixed at 1.8 ppmv while CO and O_3 were initialised at 200 and 40 ppbv and then allowed to evolve freely.

The VOCs used in this study are assigned to mechanism species following the recommendations from the literature of each mechanism (Table 1), the representation of each VOC in the mechanisms is found in Table 2. Emissions of lumped species are weighted by the carbon number of the mechanism species ensuring the total amount of emitted reactive carbon was the same in each model run.

The MECCA box model is based upon the Kinetic Pre-Processor (KPP) (Damian et al., 2002). Hence, all chemical mechanisms were adapted into modularised KPP format. The inorganic gas-phase chemistry described in the MCM v3.2 was used in each run to remove any differences between

treatments of inorganic chemistry in each mechanism. Thus, differences between the O_3 produced by the mechanisms are due to the treatment of organic degradation chemistry.

The MCM v3.2 approach to photolysis, dry deposition of VOC oxidation intermediates and RO_2−RO_2 reactions was used for each mechanism; details of these adaptations can be found in the Supplement. Some mechanisms include reactions which are only important in the stratosphere or free troposphere. For example, PAN photolysis is only important in the free troposphere (Harwood et al., 2003) and was removed from MOZART-4, RACM2 and CB05 for the purpose of the study, as this study considers processes occurring within the planetary boundary layer.

2.3 Tagged ozone production potential (TOPP)

This section summarises the tagging approach described in Butler et al. (2011) which is applied in this study.

2.3.1 O_x family and tagging approach

O_3 production and loss is dominated by rapid photochemical cycles, such as Reactions (R1)–(R3). The effects of rapid production and loss cycles can be removed by using chemical families that include rapidly inter-converting species. In this study, we define the O_x family to include O_3, $O(^3P)$, $O(^1D)$, NO_2 and other species involved in fast cycling with NO_2, such as HO_2NO_2 and PAN species. Thus, production of O_x can be used as a proxy for production of O_3.

The tagging approach follows the degradation of emitted VOCs through all possible pathways by labelling every organic degradation product with the name of the emitted VOCs. Thus, each emitted VOC effectively has its own set of degradation reactions. Butler et al. (2011) showed that O_x production can be attributed to the VOCs by following the tags of each VOC.

Table 2. Non-methane volatile organic compounds (NMVOCs) present in Los Angeles. Mixing ratios are taken from Baker et al. (2008) and their representation in each chemical mechanism. The representation of the VOCs in each mechanism is based upon the recommendations of the literature for each mechanism (Table 1).

NMVOCs	Mixing ratio (pptv)	MCM v3.1, v3.2, CRI v2	MOZART-4	RADM2	RACM	RACM2	CBM-IV	CB05
Alkanes								
Ethane	6610	C2H6	C2H6	ETH	ETH	ETH	0.4 PAR	ETHA
Propane	6050	C3H8	C3H8	HC3	HC3	HC3	1.5 PAR	1.5 PAR
Butane	2340	NC4H10	BIGALK	HC3	HC3	HC3	4 PAR	4 PAR
2-Methylpropane	1240	IC4H10	BIGALK	HC3	HC3	HC3	4 PAR	4 PAR
Pentane	1200	NC5H12	BIGALK	HC5	HC5	HC5	5 PAR	5 PAR
2-Methylbutane	2790	IC5H12	BIGALK	HC5	HC5	HC5	5 PAR	5 PAR
Hexane	390	NC6H14	BIGALK	HC5	HC5	HC5	6 PAR	6 PAR
Heptane	160	NC7H16	BIGALK	HC5	HC5	HC5	7 PAR	7 PAR
Octane	80	NC8H18	BIGALK	HC8	HC8	HC8	8 PAR	8 PAR
Alkenes								
Ethene	2430	C2H4	C2H4	OL2	ETE	ETE	ETH	ETH
Propene	490	C3H6	C3H6	OLT	OLT	OLT	OLE + PAR	OLE + PAR
Butene	65	BUT1ENE	BIGENE	OLT	OLT	OLT	OLE + 2 PAR	OLE + 2 PAR
2-Methylpropene	130	MEPROPENE	BIGENE	OLI	OLI	OLI	PAR + FORM + ALD2	FORM + 3 PAR
Isoprene	270	C5H8	ISOP	ISO	ISO	ISO	ISOP	ISOP
Aromatics								
Benzene	480	BENZENE	TOLUENE	TOL	TOL	BEN	PAR	PAR
Toluene	1380	TOLUENE	TOLUENE	TOL	TOL	TOL	TOL	TOL
m-Xylene	410	MXYL	TOLUENE	XYL	XYL	XYM	XYL	XYL
p-Xylene	210	PXYL	TOLUENE	XYL	XYL	XYP	XYL	XYL
o-Xylene	200	OXYL	TOLUENE	XYL	XYL	XYO	XYL	XYL
Ethylbenzene	210	EBENZ	TOLUENE	TOL	TOL	TOL	TOL + PAR	TOL + PAR

O_x production from lumped-mechanism species are reassigned to the VOCs of Table 2 by scaling the O_x production of the mechanism species by the fractional contribution of each represented VOC. For example, TOL in RACM2 represents toluene and ethylbenzene with fractional contributions of 0.87 and 0.13 to TOL emissions. Scaling the O_x production from TOL by these factors gives the O_x production from toluene and ethylbenzene in RACM2.

Many reduced mechanisms use an operator species as a surrogate for RO_2 during VOC degradation enabling these mechanisms to produce O_x while minimising the number of RO_2 species represented. O_x production from operator species is assigned as O_x production from the organic degradation species producing the operator. This allocation technique is also used to assign O_x production from HO_2 via Reaction (R7).

2.3.2 Definition of TOPP

Attributing O_x production to individual VOCs using the tagging approach is the basis for calculating the TOPP of a VOC, which is defined as the number of O_x molecules produced per emitted molecule of VOC. The TOPP value of a VOC that is not represented explicitly in a chemical mechanism is calculated by multiplying the TOPP value of the mechanism species representing the VOCs by the ratio of the carbon numbers of the VOCs to the mechanism species. For example, CB05 represents hexane as 6 PAR, so the TOPP value of hexane in the CB05 is 6 times the TOPP of PAR. MOZART-4 represents hexane with the five carbon species BIGALK. Thus, hexane emissions are represented molecule for molecule as $\frac{6}{5}$ of the equivalent number of molecules of BIGALK, and the TOPP value of hexane in MOZART-4 is calculated by multiplying the TOPP value of BIGALK by $\frac{6}{5}$.

3 Results

3.1 Ozone time series and O_x production budgets

Figure 1 shows the time series of O_3 mixing ratios obtained with each mechanism. There is an 8 ppbv difference in O_3 mixing ratios on the first day between RADM2, which has the highest O_3, and RACM2, which has the lowest O_3 mixing ratios when not considering the outlier time series of RACM. The difference between RADM2 and RACM, the low outlier, was 21 ppbv on the first day. The O_3 mixing ratios in
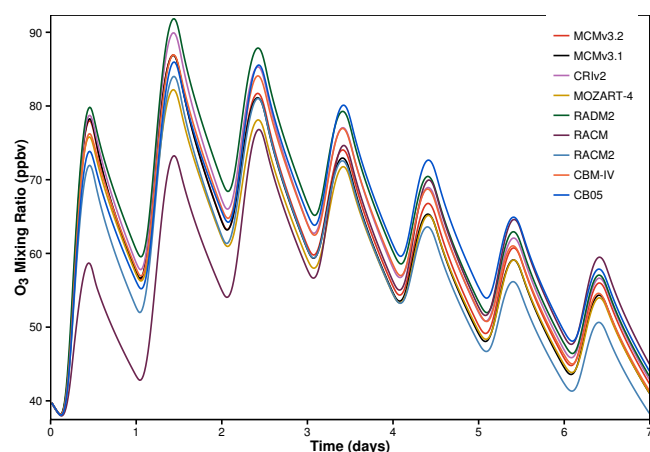
Figure 1. Time series of O_3 mixing ratios obtained using each mechanism.

Figure 2. Day-time O_x production budgets in each mechanism allocated to individual VOCs.

the CRI v2 are larger than those in the MCM v3.1, which is similar to the results in Jenkin et al. (2008) where the O_3 mixing ratios of the CRI v2 and MCM v3.1 are compared over a 5-day period.

The O_3 mixing ratios in Fig. 1 are influenced by the approaches used in developing the chemical mechanisms and not a function of the explicitness of the chemical mechanism. For example, the O_3 mixing ratios obtained using the Carbon Bond mechanisms (CBM-IV and CB05) compare well with the MCM despite both Carbon Bond mechanisms having $\sim 1\%$ of the number of reactions in the MCM v3.2. Also, the O_3 mixing ratios from RACM2 and RADM2 show similar absolute differences from that of the MCM despite RACM2 having more than double the number of reactions of RADM2.

The day-time O_x production budgets allocated to individual VOCs for each mechanism are shown in Fig. 2. The relationships between O_3 mixing ratios in Fig. 1 are mirrored in Fig. 2 where mechanisms producing high amounts of O_x also have high O_3 mixing ratios. The conditions in the box model lead to a daily maximum of OH that increases with each day leading to an increase on each day in both the reaction rate of the OH oxidation of CH_4 and the daily contribution of CH_4 to O_x production.

The first-day mixing ratios of O_3 in RACM are lower than other mechanisms due to a lack of O_x production from aromatic VOCs on the first day in RACM (Fig. 2). Aromatic degradation chemistry in RACM results in net loss of O_x on the first day, described later in Sect. 3.2.1.

RADM2 is the only reduced mechanism that produces higher O_3 mixing ratios than the more detailed mechanisms (MCM v3.2, MCM v3.1 and CRI v2). Higher mixing ratios of O_3 in RADM2 are produced due to increased O_x production from propane compared to the MCM v3.2; on the first day, the O_x production from propane in RADM2 is triple that of the MCM v3.2 (Fig. 2). Propane is represented as HC3 in
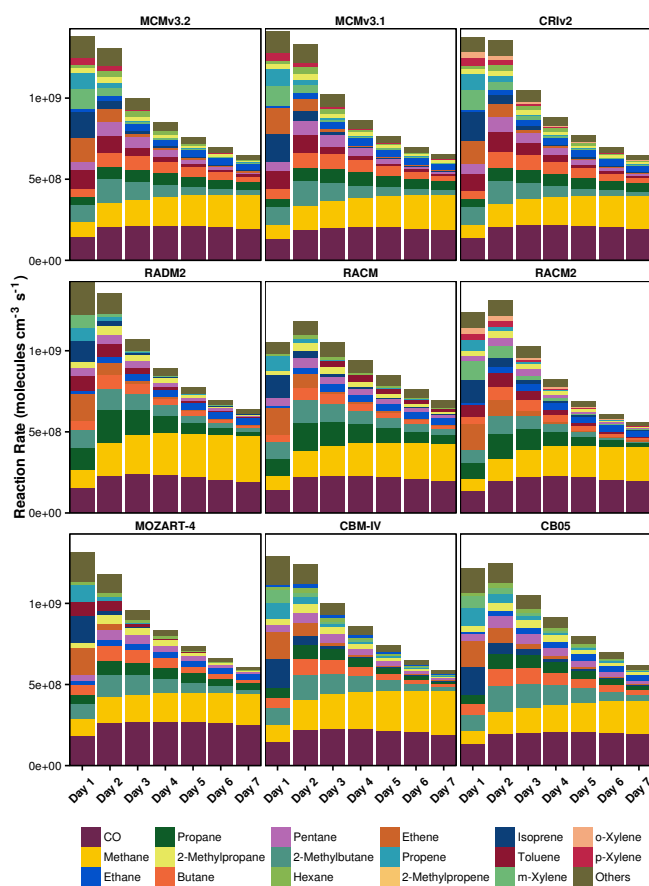
RADM2 (Stockwell et al., 1990) and the degradation of HC3 has a lower yield of the less-reactive ketones compared to the MCM. The further degradation of ketones hinders O_x production due to the low OH reactivity and photolysis rate of ketones. Secondary degradation of HC3 proceeds through the degradation of acetaldehyde (CH_3CHO) propagating O_x production through the reactions of CH_3CO_3 and CH_3O_2 with NO. Thus, the lower ketone yields lead to increased O_x production from propane degradation in RADM2 compared to the MCM v3.2.

3.2 Time-dependent O_x production

Time series of daily TOPP values for each VOC are presented in Fig. 3 and the cumulative TOPP values at the end of the model run obtained for each VOC using each of the mechanisms, normalised by the number of atoms of C in each VOC are presented in Table 3. In the MCM and CRI v2, the cumulative TOPP values obtained for each VOC show that by the end of the model run, larger alkanes have produced more O_x per unit of reactive C than alkenes or aromatic VOCs. By the end of the runs using the lumped-structure mechanisms (CBM-IV and CB05), alkanes produce similar
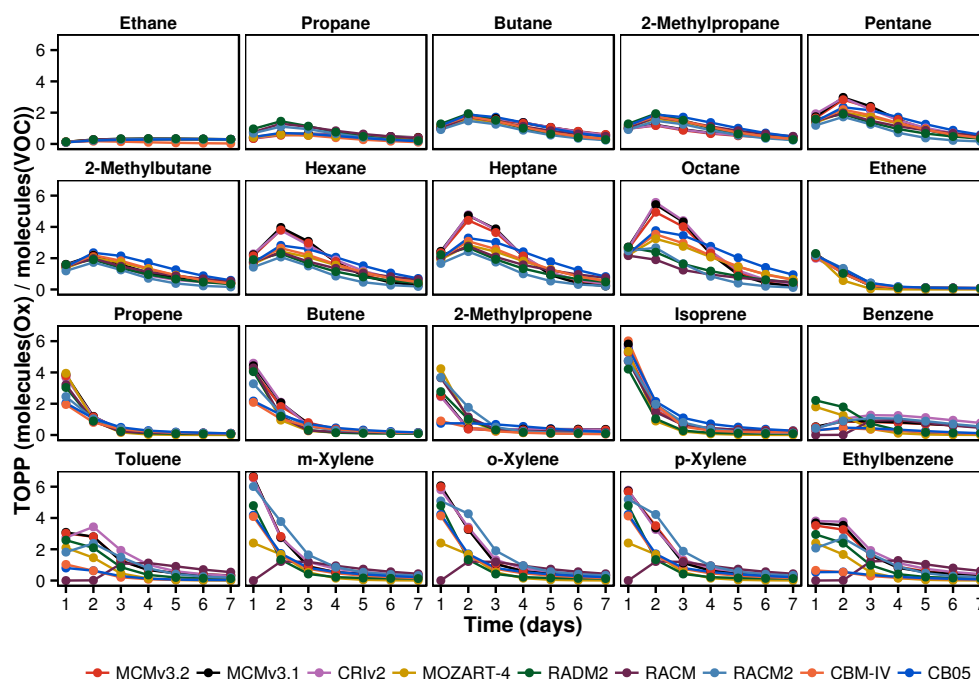
Figure 3. TOPP value time series using each mechanism for each VOC.

Table 3. Cumulative TOPP values at the end of the model run for all VOCs with each mechanism, normalised by the number of C atoms in each VOC.

NMVOCs	MCM v3.2	MCM v3.1	CRI v2	MOZART-4	RADM2	RACM	RACM2	CBM-IV	CB05
Alkanes									
Ethane	0.9	1.0	0.9	0.9	1.0	1.0	0.9	0.3	0.9
Propane	1.1	1.2	1.2	1.1	1.8	1.8	1.4	0.9	1.0
Butane	2.0	2.0	2.0	1.7	1.8	1.8	1.4	1.7	2.1
2-Methylpropane	1.3	1.3	1.3	1.7	1.8	1.8	1.4	1.7	2.1
Pentane	2.1	2.1	2.2	1.7	1.5	1.6	1.1	1.7	2.1
2-Methylbutane	1.6	1.6	1.5	1.7	1.5	1.6	1.1	1.7	2.1
Hexane	2.1	2.1	2.2	1.7	1.5	1.6	1.1	1.7	2.1
Heptane	2.0	2.1	2.2	1.7	1.5	1.6	1.1	1.7	2.1
Octane	2.0	2.0	2.2	1.7	1.2	1.0	1.0	1.7	2.1
Alkenes									
Ethene	1.9	1.9	1.9	1.4	2.0	2.0	2.2	1.9	2.2
Propene	1.9	2.0	1.9	1.7	1.5	1.6	1.5	1.2	1.4
Butene	1.9	2.0	2.0	1.5	1.5	1.6	1.5	0.8	0.9
2-Methylpropene	1.1	1.2	1.2	1.5	1.1	1.5	1.6	0.5	0.5
Isoprene	1.8	1.8	1.8	1.3	1.2	1.6	1.7	1.9	2.1
Aromatics									
Benzene	0.8	0.8	1.1	0.6	0.9	0.6	0.9	0.3	0.3
Toluene	1.3	1.3	1.5	0.6	0.9	0.6	1.0	0.3	0.3
m-Xylene	1.5	1.5	1.6	0.6	0.9	0.6	1.7	0.9	1.0
p-Xylene	1.5	1.5	1.6	0.6	0.9	0.6	1.7	0.9	1.0
o-Xylene	1.5	1.5	1.6	0.6	0.9	0.6	1.7	0.9	1.0
Ethylbenzene	1.3	1.4	1.5	0.6	0.9	0.6	1.0	0.2	0.3

amounts of O_x per reactive C, while aromatic VOCs and some alkenes produce less O_x per reactive C than the MCM. However, in lumped-molecule mechanisms (MOZART-4, RADM2, RACM, RACM2), practically all VOCs produce less O_x per reactive C than the MCM by the end of the run. This lower efficiency of O_x production from many individual VOCs in lumped-molecule and lumped-structure mechanisms would lead to an underestimation of O_3 levels downwind of an emission source, and a smaller contribution to background O_3 when using lumped-molecule and lumped-structure mechanisms.

The lumped-intermediate mechanism (CRI v2) produces the most similar O_x to the MCM v3.2 for each VOC, seen in Fig. 3 and Table 3. Higher variability in the time-dependent O_x production is evident for VOCs represented by lumped-mechanism species. For example, 2-methylpropene, represented in the reduced mechanisms by a variety of lumped species, has a higher spread in time-dependent O_x production than ethene, which is explicitly represented in each mechanism.

In general, the largest differences in O_x produced by aromatic and alkene species are on the first day of the simulations, while the largest inter-mechanism differences in O_x produced by alkanes are on the second and third days of the simulations. The reasons for these differences in behaviour will be explored in Sect. 3.2.1, which examines differences in first day O_x production between the chemical mechanisms, and Sect. 3.2.2, which examines the differences in O_x production on subsequent days.

3.2.1 First-day ozone production

The first-day TOPP values of each VOC from each mechanism, representing O_3 production from freshly emitted VOCs near their source region, are compared to those obtained with the MCM v3.2 in Fig. 4. The root mean square error (RMSE) of all first-day TOPP values in each mechanism relative to those in the MCM v3.2 are also included in Fig. 4. The RMSE value of the CRI v2 shows that first-day O_x production from practically all the individual VOC matches that in the MCM v3.2. All other reduced mechanisms have much larger RMSE values indicating that the first-day O_x production from the majority of the VOCs differs from that in the MCM v3.2.

The reduced complexity of reduced mechanisms means that aromatic VOCs are typically represented by one or two mechanism species leading to differences in O_x production of the actual VOCs compared to the MCM v3.2. For example, all aromatic VOCs in MOZART-4 are represented as toluene, thus less-reactive aromatic VOCs, such as benzene, produce higher O_x whilst more-reactive aromatic VOCs, such as the xylenes, produce less O_x in MOZART-4 than the MCM v3.2. RACM2 includes explicit species representing benzene, toluene and each xylene resulting in O_x production
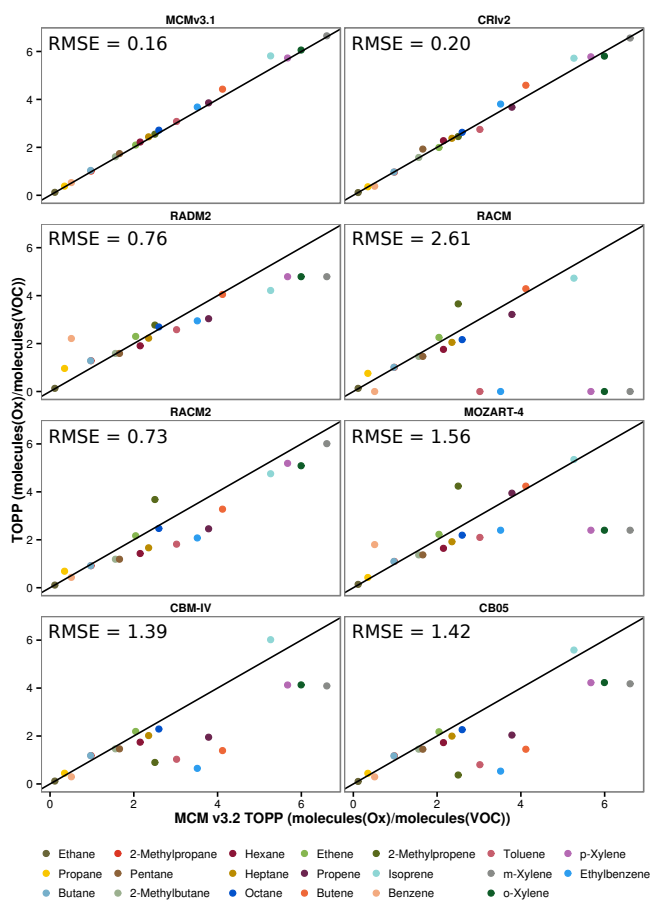

Figure 4. The first-day TOPP values for each VOC calculated using MCM v3.2 and the corresponding values in each mechanism. The root mean square error (RMSE) of each set of TOPP values is also displayed. The black line is the 1 : 1 line.

that is the most similar to the MCM v3.2 than other reduced mechanisms.

Figure 3 shows a high spread in O_x production from aromatic VOCs on the first day indicating that aromatic degradation is treated differently between mechanisms. Toluene degradation is examined in more detail by comparing the reactions contributing to O_x production and loss in each mechanism, shown in Fig. 5. These reactions are determined by following the "toluene" tags in the tagged version of each mechanism.

Toluene degradation in RACM includes several reactions consuming O_x that are not present in the MCM, resulting in net loss of O_x on the first 2 days. Ozonolysis of the cresol OH adduct mechanism species, ADDC, contributes significantly to O_x loss in RACM. This reaction was included in RACM due to improved cresol product yields when comparing RACM predictions with experimental data (Stockwell et al., 1997). Other mechanisms that include cresol OH adduct species do not include ozonolysis and these reactions are not included in the updated RACM2.
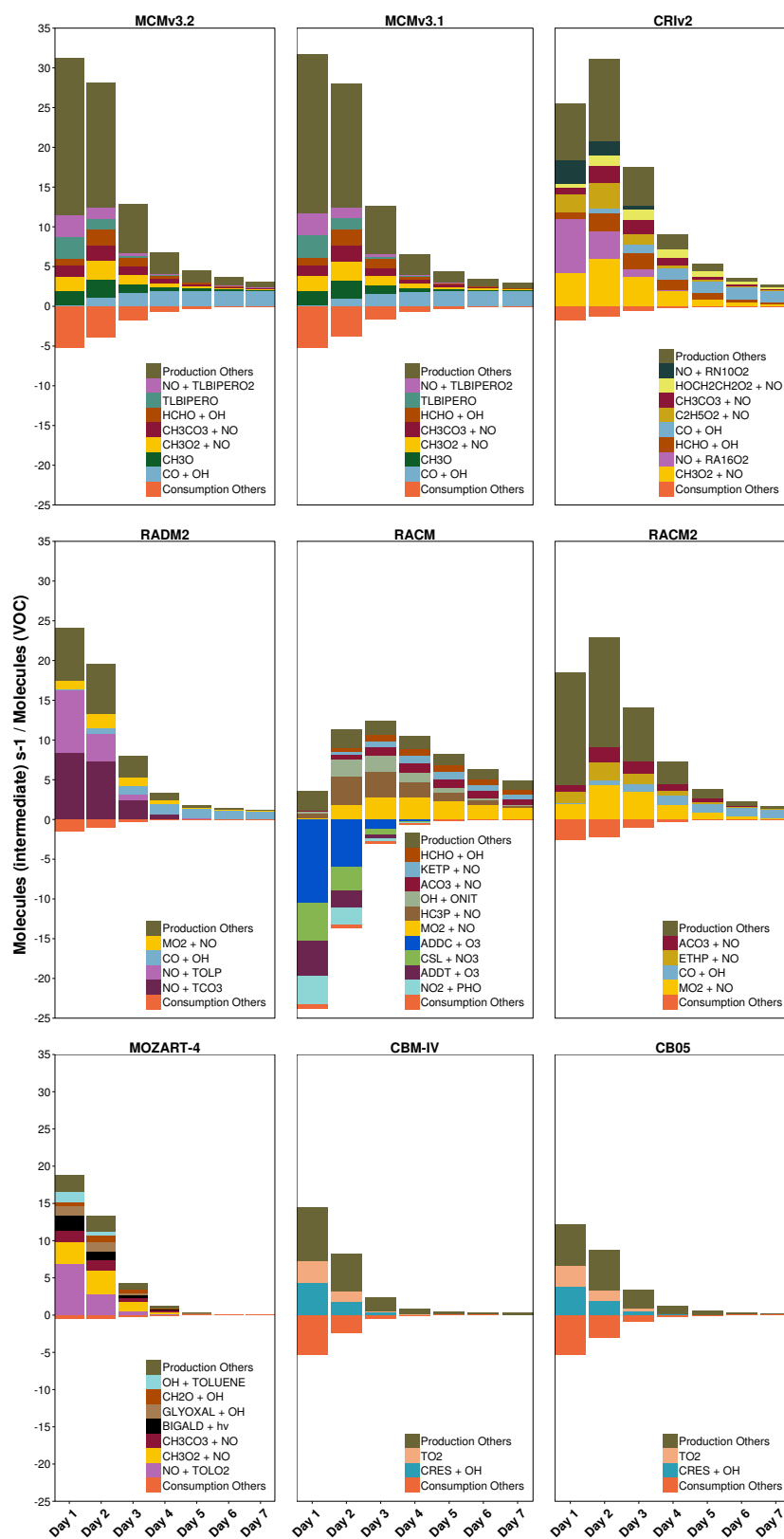
Figure 5. Day-time O_x production and loss budgets allocated to the responsible reactions during toluene degradation in all mechanisms. These reactions are presented using the species defined in each mechanism in Table 1.

The total O_x produced on the first day during toluene degradation in each reduced mechanism is less than that in the MCM v3.2 (Fig. 5). Less O_x is produced in all reduced mechanisms due to a faster breakdown of the VOCs into smaller fragments than the MCM, described later in Sect. 3.3. Moreover, in CBM-IV and CB05, less O_x is produced during toluene degradation as reactions of the toluene degradation products CH_3O_2 and CO do not contribute to the O_x production budgets, which is not the case in any other mechanism (Fig. 5).

Maximum O_x production from toluene degradation in CRI v2 and RACM2 is reached on the second day in contrast to the MCM v3.2 which produces peak O_x on the first day. The second-day maximum of O_x production in CRI v2 and RACM2 from toluene degradation results from more efficient production of unsaturated dicarbonyls than the MCM v3.2. The degradation of unsaturated dicarbonyls produces peroxy radicals such as $C_2H_5O_2$ which promote O_x production via reactions with NO.

Unsaturated aliphatic VOCs generally produce similar amounts of O_x between mechanisms, especially explicitly represented VOCs, such as ethene and isoprene. On the other hand, unsaturated aliphatic VOCs that are not explicitly represented produce differing amounts of O_x between mechanisms (Fig. 3). For example, the O_x produced during 2-methylpropene degradation varies between mechanisms; differing rate constants of initial oxidation reactions and non-realistic secondary chemistry lead to these differences; further details are found in the Supplement.

Non-explicit representations of aromatic and unsaturated aliphatic VOCs coupled with differing degradation chemistry and a faster breakdown into smaller-size degradation products results in different O_x production in lumped-molecule and lumped-structure mechanisms compared to the MCM v3.2.

3.2.2 Ozone production on subsequent days

Alkane degradation in CRI v2 and both MCMs produces a second-day maximum in O_x that increases with alkane carbon number (Fig. 3). The increase in O_x production on the second day is reproduced for each alkane by the reduced mechanisms, except octane in RADM2, RACM and RACM2. However, larger alkanes produce less O_x than the MCM on the second day in all lumped-molecule and lumped-structure mechanisms.

The lumped-molecule mechanisms (MOZART-4, RADM2, RACM and RACM2) represent many alkanes by mechanism species which may lead to unrepresentative secondary chemistry for alkane degradation. For example, 3 times more O_x is produced during the degradation of propane in RADM2 than the MCM v3.2 on the first day (Fig. 2). Propane is represented in RADM2 by the mechanism species HC3 which also represents other classes of VOCs, such as alcohols. The secondary chemistry of HC3 is
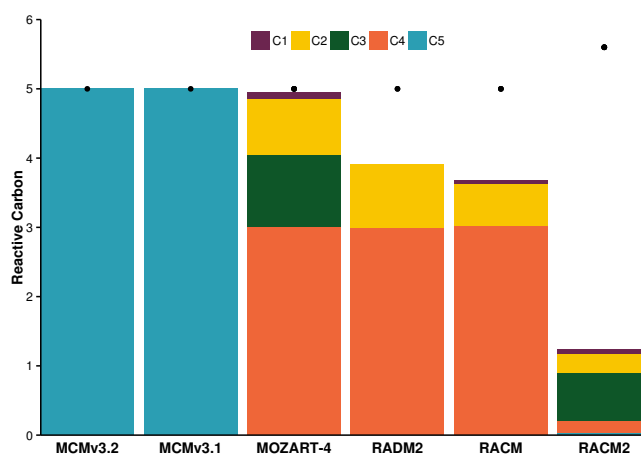

Figure 6. The distribution of reactive carbon in the products of the reaction between NO and the pentyl peroxy radical in lumped-molecule mechanisms compared to the MCM. The black dot represents the reactive carbon of the pentyl peroxy radical.

tailored to produce O_x from these different VOCs and differs from alkane degradation in the MCM v3.2 by producing less ketones in RADM2.

As will be shown in Sect. 3.3, another feature of reduced mechanisms is that the breakdown of emitted VOCs into smaller-sized degradation products is faster than the MCM. Alkanes are broken down quicker in CBM-IV, CB05, RADM2, RACM and RACM2 through a higher rate of reactive carbon loss than the MCM v3.2 (shown for pentane and octane in Fig. 8); reactive carbon is lost through reactions not conserving carbon. Despite many degradation reactions of alkanes in MOZART-4 almost conserving carbon, the organic products have less reactive carbon than the organic reactant also speeding up the breakdown of the alkane compared to the MCM v3.2.

For example, Fig. 6 shows the distribution of reactive carbon in the reactants and products from the reaction of NO with the pentyl peroxy radical in both MCMs and each lumped-molecule mechanism. In all the lumped-molecule mechanisms, the individual organic products have less reactive carbon than the organic reactant. Moreover, in RADM2, RACM and RACM2, this reaction does not conserve reactive carbon leading to faster loss rates of reactive carbon.

The faster breakdown of alkanes in lumped-molecule and lumped-structure mechanisms on the first day limits the amount of O_x produced on the second day, as less of the larger-sized degradation products are available for further degradation and O_x production.

3.3 Treatment of degradation products

The time-dependent O_x production of the different VOCs in Fig. 3 results from the varying rates at which VOCs break up into smaller fragments (Butler et al., 2011). Varying breakdown rates of the same VOCs between mechanisms could

Figure 7. Day-time O_x production during pentane and toluene degradation is attributed to the number of carbon atoms of the degradation products for each mechanism.

explain the different time-dependent O_x production between mechanisms. The breakdown of pentane and toluene between mechanisms is compared in Fig. 7 by allocating the O_x production to the number of carbon atoms in the degradation products responsible for O_x production on each day of the model run in each mechanism. Some mechanism species in RADM2, RACM and RACM2 have fractional carbon numbers (Stockwell et al., 1990, 1997; Goliff et al., 2013) and O_x production from these species was reassigned as O_x production of the nearest integral carbon number.

The degradation of pentane, a five-carbon VOC, on the first day in the MCM v3.2 produces up to 50 % more O_x from degradation products also having five carbon atoms than any reduced mechanism. Moreover, the contribution of the degradation products having five carbon atoms in the MCM v3.2 is consistently higher throughout the model run than in re-

duced mechanisms (Fig. 7). Despite producing less total O_x, reduced mechanisms produce up to double the amount of O_x from degradation products with one carbon atom than in the MCM v3.2. The lower contribution of larger degradation products indicates that pentane is generally broken down faster in reduced mechanisms, consistent with the specific example shown for the breakdown of the pentyl peroxy radical in Fig. 6.

The rate of change in reactive carbon during pentane, octane and toluene degradation was determined by multiplying the rate of each reaction occurring during pentane, octane and toluene degradation by its net change in carbon, shown in Fig. 8. Pentane is broken down faster in CBM-IV, CB05, RADM2, RACM and RACM2 by losing reactive carbon more quickly than the MCM v3.2. MOZART-4 also breaks pentane down into smaller-sized products quicker

Figure 8. Daily rate of change in reactive carbon during pentane, octane and toluene degradation. Octane is represented by the five carbon species, BIGALK, in MOZART-4.

than the MCM v3.2 as reactions during pentane degradation in MOZART-4 have organic products whose carbon number is less than the organic reactant, described in Sect. 3.2.2. The faster breakdown of pentane on the first day limits the amount of reactive carbon available to produce further O_x on subsequent days leading to lower O_x production after the first day in reduced mechanisms.

Figure 3 showed that octane degradation produces peak O_x on the first day in RADM2, RACM and RACM2 in contrast to all other mechanisms where peak O_x is produced on the second day. Octane degradation in RADM2, RACM and RACM2 loses reactive carbon much faster than any other mechanism on the first day so that there are not enough degradation products available to produce peak O_x on the second day (Fig. 8). This loss of reactive carbon during alkane degradation leads to the lower accumulated ozone production from these VOCs shown in Table 3.

As seen in Fig. 3, O_x produced during toluene degradation has a high spread between the mechanisms. Figure 7 shows differing distributions of the sizes of the degradation products that produce O_x. All reduced mechanisms omit O_x production from at least one degradation fragment size which produces O_x in the MCM v3.2, indicating that toluene is also broken down more quickly in the reduced mechanisms than the more explicit mechanisms. For example, toluene degradation in RACM2 does not produce O_x from degradation products with six carbons, as is the case in the MCM v3.2. Figure 8 shows that all reduced mechanisms lose reactive carbon during toluene degradation faster than the MCM v3.2. Thus, the degradation of aromatic VOCs in reduced mechanisms are unable to produce similar amounts of O_x as the explicit mechanisms.

4   Conclusions

Tagged ozone production potentials (TOPPs) were used to compare O_x production during VOC degradation in reduced chemical mechanisms to the near-explicit MCM v3.2. First-day mixing ratios of O_3 are similar to the MCM v3.2 for most mechanisms; the O_3 mixing ratios in RACM were much lower than the MCM v3.2 due to a lack of O_x production from the degradation of aromatic VOCs. Thus, RACM may not be the appropriate chemical mechanism when simulating atmospheric conditions having a large fraction of aromatic VOCs.

The lumped-intermediate mechanism, CRI v2, produces the most similar amounts of O_x to the MCM v3.2 for each VOC. The largest differences between O_x production in CRI v2 and MCM v3.2 were obtained for aromatic VOCs; however, overall these differences were much lower than any other reduced mechanism. Thus, when developing chemical mechanisms, the technique of using lumped-intermediate species whose degradation are based upon more detailed mechanism should be considered.

Many VOCs are broken down into smaller-sized degradation products faster on the first day in reduced mechanisms than the MCM v3.2 leading to lower amounts of larger-sized degradation products that can further degrade and produce O_x. Thus, many VOCs in reduced mechanisms produce a lower maximum of O_x and lower total O_x per reactive C by the end of the run than the MCM v3.2. This lower O_x production from many VOCs in reduced mechanisms leads to lower O_3 mixing ratios compared to the MCM v3.2.

Alkanes produce maximum O_3 on the second day of simulations and this maximum is lower in reduced mechanisms than the MCM v3.2 due to the faster breakdown of alkanes into smaller-sized degradation products on the first day. The lower maximum in O_3 production during alkane degradation in reduced mechanisms leads to an underestimation of the O_3 levels downwind of VOC emissions and an underestimation of the VOC contribution to tropospheric background O_3 when using reduced mechanisms in regional or global modelling studies.

This study has determined the maximum potential of VOCs represented in reduced mechanisms to produce O_3; this potential may not be reached as ambient NO_x conditions may not induce NO_x–VOC-sensitive chemistry. Moreover, the maximum potential of VOCs to produce O_3 may not be reached when using these reduced mechanisms in 3-D models due to the influence of additional processes, such as mixing and meteorology. Future work shall examine the extent to which the maximum potential of VOCs to produce O_3 in reduced chemical mechanisms is reached using ambient NO_x conditions and including processes found in 3-D models.

References

Ahmadov, R., McKeen, S., Trainer, M., Banta, R., Brewer, A., Brown, S., Edwards, P. M., de Gouw, J. A., Frost, G. J., Gilman, J., Helmig, D., Johnson, B., Karion, A., Koss, A., Langford, A., Lerner, B., Olson, J., Oltmans, S., Peischl, J., Pétron, G., Pichugina, Y., Roberts, J. M., Ryerson, T., Schnell, R., Senff, C., Sweeney, C., Thompson, C., Veres, P. R., Warneke, C., Wild, R., Williams, E. J., Yuan, B., and Zamora, R.: Understanding high wintertime ozone pollution events in an oil- and natural gas-producing region of the western US, Atmos. Chem. Phys., 15, 411–429, doi:10.5194/acp-15-411-2015, 2015.

Atkinson, R.: Atmospheric chemistry of VOCs and NO_x, Atmos. Environ., 34, 2063–2101, 2000.

Baker, A. K., Beyersdorf, A. J., Doezema, L. A., Katzenstein, A., Meinardi, S., Simpson, I. J., Blake, D. R., and Rowland, F. S.: Measurements of nonmethane hydrocarbons in 28 United States cities, Atmos. Environ., 42, 170–182, 2008.

Baklanov, A., Schlünzen, K., Suppan, P., Baldasano, J., Brunner, D., Aksoyoglu, S., Carmichael, G., Douros, J., Flemming, J., Forkel, R., Galmarini, S., Gauss, M., Grell, G., Hirtl, M., Joffre, S., Jorba, O., Kaas, E., Kaasik, M., Kallos, G., Kong, X., Korsholm, U., Kurganskiy, A., Kushta, J., Lohmann, U., Mahura, A., Manders-Groot, A., Maurizi, A., Moussiopoulos, N., Rao, S. T., Savage, N., Seigneur, C., Sokhi, R. S., Solazzo, E., Solomos, S., Sørensen, B., Tsegas, G., Vignati, E., Vogel, B., and Zhang, Y.: Online coupled regional meteorology chemistry models in Europe: current status and prospects, Atmos. Chem. Phys., 14, 317–398, doi:10.5194/acp-14-317-2014, 2014.

Bloss, C., Wagner, V., Jenkin, M. E., Volkamer, R., Bloss, W. J., Lee, J. D., Heard, D. E., Wirtz, K., Martin-Reviejo, M., Rea, G., Wenger, J. C., and Pilling, M. J.: Development of a detailed chemical mechanism (MCMv3.1) for the atmospheric oxidation of aromatic hydrocarbons, Atmos. Chem. Phys., 5, 641–664, doi:10.5194/acp-5-641-2005, 2005.

Butler, T. M., Lawrence, M. G., Taraborrelli, D., and Lelieveld, J.: Multi-day ozone production potential of volatile organic compounds calculated with a tagging approach, Atmos. Environ., 45, 4082–4090, 2011.

Carter, W. P. L.: Development of ozone reactivity scales for volatile organic compounds, J. Air Waste Manage., 44, 881–899, 1994.

Damian, V., Sandu, A., Damian, M., Potra, F., and Carmichael, G.: The kinetic preprocessor KPP – a software environment for solving chemical kinetics, Comput. Chem. Eng., 26, 1567–1579, 2002.

Derwent, R. G., Jenkin, M. E., and Saunders, S. M.: Photochemical ozone creation potentials for a large number of reactive hydrocarbons under European conditions, Atmos. Environ., 30, 181–199, 1996.

Derwent, R. G., Jenkin, M. E., Saunders, S. M., and Pilling, M. J.: Photochemical ozone creation potentials for organic compounds in Northwest Europe calculated with a master chemical mechanism, Atmos. Environ., 32, 2429–2441, 1998.

Derwent, R. G., Jenkin, M. E., Pilling, M. J., Carter, W. P. L., and Kaduwela, A.: Reactivity scales as comparative tools for chemical mechanisms, J. Air Waste Manage., 60, 914–924, 2010.

Derwent, R. G., Utember, S. R., Jenkin, M. E., and Shallcross, D. E.: Tropospheric ozone production regions and the intercontinental origins of surface ozone over Europe, Atmos. Environ., 112, 216–224, 2015

Dodge, M.: Chemical oxidant mechanisms for air quality modeling: critical review, Atmos. Environ., 34, 2103–2130, 2000.

Dunker, A. M., Kumar, S., and Berzins, P. H.: A comparison of chemical mechanisms used in atmospheric models, Atmos. Environ., 18, 311–321, 1984.

Dunker, A. M., Koo, B., and Yarwood, G.: Source Apportionment of the Anthropogenic Increment to Ozone, Formaldehyde, and Nitrogen Dioxide by the Path- Integral Method in a 3D Model, Environ. Sci. Technol., 49, 6751–6759, 2015.

EEA: Air quality in Europe – 2014 report, Tech. Rep. 5/2014, European Environmental Agency, Publications Office of the European Union, doi:10.2800/22847, 2014.

Emmerson, K. M. and Evans, M. J.: Comparison of tropospheric gas-phase chemistry schemes for use within global models, Atmos. Chem. Phys., 9, 1831–1845, doi:10.5194/acp-9-1831-2009, 2009.

Emmons, L. K., Walters, S., Hess, P. G., Lamarque, J.-F., Pfister, G. G., Fillmore, D., Granier, C., Guenther, A., Kinnison, D., Laepple, T., Orlando, J., Tie, X., Tyndall, G., Wiedinmyer, C., Baughcum, S. L., and Kloster, S.: Description and evaluation of the Model for Ozone and Related chemical Tracers, version 4 (MOZART-4), Geosci. Model Dev., 3, 43–67, doi:10.5194/gmd-3-43-2010, 2010.

Foster, P. N., Prentice, I. C., Morfopoulos, C., Siddall, M., and van Weele, M.: Isoprene emissions track the seasonal cycle of canopy temperature, not primary production: evidence from remote sensing, Biogeosciences, 11, 3437–3451, doi:10.5194/bg-11-3437-2014, 2014.

Gery, M. W., Whitten, G. Z., Killus, J. P., and Dodge, M. C.: A photochemical kinetics mechanism for urban and regional scale computer modeling, J. Geophys. Res., 94, 12925–12956, 1989.

Goliff, W. S., Stockwell, W. R., and Lawson, C. V.: The regional atmospheric chemistry mechanism, version 2, Atmos. Environ., 68, 174–185, 2013.

Goliff, W. S., Luria, M., Blake, D. R., Zielinska, B., Hallar, G., Valente, R. J., Lawson, C. V., and Stockwell, W. R.: Nighttime air quality under desert conditions, Atmos. Environ., 114, 102–111, 2015.

Harwood, M., Roberts, J., Frost, G., Ravishankara, A., and Burkholder, J.: Photochemical studies of $CH_3C(O)OONO_2$ (PAN) and $CH_3CH_2C(O)OONO_2$ (PPN): NO_3 quantum yields, J. Phys. Chem. A, 107, 1148–1154, 2003.

Hogo, H. and Gery, M.: User's guide for executing OZIPM-4 (Ozone Isopleth Plotting with Optional Mechanisms, Version 4) with CBM-IV (Carbon-Bond Mechanisms-IV) or optional mechanisms. Volume 1. Description of the ozone isopleth plotting package. Version 4, Tech. rep., US Environmental Protection Agency, Durham, North Carolina, USA, 1989.

Hou, X., Zhu, B., Fei, D., and Wang, D.: The impacts of summer monsoons on the ozone budget of the atmospheric boundary

layer of the Asia-Pacific region, Sci. Total Environ., 502, 641–649, 2015.

HTAP: Hemispheric Transport of Air Pollution 2010, Part A: Ozone and Particulate Matter, Air Pollution Studies No.17, Geneva, Switzerland, 2010.

Jenkin, M. E. and Clemitshaw, K. C.: Ozone and other secondary photochemical pollutants: chemical processes governing their formation in the planetary boundary layer, Atmos. Environ., 34, 2499–2527, 2000.

Jenkin, M. E., Saunders, S. M., and Pilling, M. J.: The tropospheric degradation of volatile organic compounds: a protocol for mechanism development, Atmos. Environ., 31, 81–104, 1997.

Jenkin, M. E., Saunders, S. M., Wagner, V., and Pilling, M. J.: Protocol for the development of the Master Chemical Mechanism, MCM v3 (Part B): tropospheric degradation of aromatic volatile organic compounds, Atmos. Chem. Phys., 3, 181–193, doi:10.5194/acp-3-181-2003, 2003.

Jenkin, M. E., Watson, L. A., Utembe, S. R., and Shallcross, D. E.: A Common Representative Intermediates (CRI) mechanism for VOC degradation. Part 1: Gas phase mechanism development, Atmos. Environ., 42, 7185–7195, 2008.

Kleinman, L. I.: Seasonal dependence of boundary layer peroxide concentration: the low and high NO_x regimes, J. Geophys. Res., 96, 20721–20733, 1991.

Kleinman, L. I.: Low and high NO_x tropospheric photochemistry, J. Geophys. Res., 99, 16831–16838, 1994.

Koss, A. R., de Gouw, J., Warneke, C., Gilman, J. B., Lerner, B. M., Graus, M., Yuan, B., Edwards, P., Brown, S. S., Wild, R., Roberts, J. M., Bates, T. S., and Quinn, P. K.: Photochemical aging of volatile organic compounds associated with oil and natural gas extraction in the Uintah Basin, UT, during a wintertime ozone formation event, Atmos. Chem. Phys., 15, 5727–5741, doi:10.5194/acp-15-5727-2015, 2015.

Kuhn, M., Builtjes, P. J. H., Poppe, D., Simpson, D., Stockwell, W. R., Andersson-Sköld, Y., Baart, A., Das, M., Fiedler, F., Hov, Ø., Kirchner, F., Makar, P. A., Milford, J. B., Roemer, M. G. M., Ruhnke, R., Strand, A., Vogel, B., and Vogel, H.: Intercomparison of the gas-phase chemistry in several chemistry and transport models, Atmos. Environ., 32, 693–709, 1998.

Li, J., Georgescu, M., Hyde, P., Mahalov, A., and Moustaoui, M.: Achieving accurate simulations of urban impacts on ozone at high resolution, Environ. Res. Lett., 9, 114019, doi:10.1088/1748-9326/9/11/114019, 2014.

Lidster, R. T., Hamilton, J. F., Lee, J. D., Lewis, A. C., Hopkins, J. R., Punjabi, S., Rickard, A. R., and Young, J. C.: The impact of monoaromatic hydrocarbons on OH reactivity in the coastal UK boundary layer and free troposphere, Atmos. Chem. Phys., 14, 6677–6693, doi:10.5194/acp-14-6677-2014, 2014.

Rickard, A., Young, J., Pilling, M., Jenkin. M., Pascoe, S., and Saunders S.: The Master Chemical Mechanism Version MCM v3.2, available at: http://mcm.leeds.ac.uk/MCMv3.2/, last access: 15 July 2015.

Sander, R., Kerkweg, A., Jöckel, P., and Lelieveld, J.: Technical note: The new comprehensive atmospheric chemistry module MECCA, Atmos. Chem. Phys., 5, 445–450, doi:10.5194/acp-5-445-2005, 2005.

Saunders, S. M., Jenkin, M. E., Derwent, R. G., and Pilling, M. J.: Protocol for the development of the Master Chemical Mechanism, MCM v3 (Part A): tropospheric degradation of non-aromatic volatile organic compounds, Atmos. Chem. Phys., 3, 161–180, doi:10.5194/acp-3-161-2003, 2003.

Sillman, S.: The relation between ozone, NO_x and hydrocarbons in urban and polluted rural environments, Atmos. Environ., 33, 1821–1845, 1999.

Stevenson, D. S., Young, P. J., Naik, V., Lamarque, J.-F., Shindell, D. T., Voulgarakis, A., Skeie, R. B., Dalsoren, S. B., Myhre, G., Berntsen, T. K., Folberth, G. A., Rumbold, S. T., Collins, W. J., MacKenzie, I. A., Doherty, R. M., Zeng, G., van Noije, T. P. C., Strunk, A., Bergmann, D., Cameron-Smith, P., Plummer, D. A., Strode, S. A., Horowitz, L., Lee, Y. H., Szopa, S., Sudo, K., Nagashima, T., Josse, B., Cionni, I., Righi, M., Eyring, V., Conley, A., Bowman, K. W., Wild, O., and Archibald, A.: Tropospheric ozone changes, radiative forcing and attribution to emissions in the Atmospheric Chemistry and Climate Model Intercomparison Project (ACCMIP), Atmos. Chem. Phys., 13, 3063–3085, doi:10.5194/acp-13-3063-2013, 2013.

Stockwell, W. R., Middleton, P., Chang, J. S., and Tang, X.: The second generation regional acid deposition model chemical mechanism for regional air quality modeling, J. Geophys. Res., 95, 16343–16367, 1990.

Stockwell, W. R., Kirchner, F., Kuhn, M., and Seefeld, S.: A new mechanism for regional atmospheric chemistry modeling, J. Geophys. Res.-Atmos., 102, 25847–25879, 1997.

Watson, L. A., Shallcross, D. E., Utembe, S. R., and Jenkin, M. E.: A Common Representative Intermediates (CRI) mechanism for VOC degradation. Part 2: Gas phase mechanism reduction, Atmos. Environ., 42, 7196–7204, 2008.

Yarwood, G., Rao, S., Yocke, M., and Whitten, G. Z.: Updates to the Carbon Bond Chemical Mechanism: CB05, Tech. rep., US Environmental Protection Agency, Novato, California, USA, 2005.

Chapter 7

Paper 2:

Chapter 8

Paper 3:

Chapter 9

Publication List

Appendix